Project No. 609687

FP7-ENERGY-2013-IRP

ELECTRA

European Liaison on Electricity Committed Towards long-term Research Activities for Smart Grids

WP 6

Control schemes for the use of flexibility

Deliverable 6.3

Core functions of the Web-of-Cells control scheme

03/01/2018

ID&Title	**D6.3** Core functions of Web-of-Cells control scheme	**Number of pages:**	48

Short description (Max. 50 words):

In order to maintain frequency (balancing) and voltage control in the future power system, the ELECTRA Web-of-Cells (WoC) control scheme introduces six high-level use cases, which are Balance Restoration Control (BRC), Frequency Containment Control (FCC), Inertia Response Power Control (IRPC), Balance Steering Control (BSC), Primary Voltage Control (PVC) and Post Primary Voltage Control (PPVC). This document presents the detailed description of the core functions that are needed and sufficient for controlling the grid in a Web-of-Cells architecture.

Version	Date	Modification's nature
V0.1	30/06/2017	First Draft
V1.00	03/07/2017	Submitted for internal TOQA Review
V1.01	15/10/2017	Submitted for internal TOQA Review, 2nd round
V1.02	21/11/2017	Final Draft
V2.00	03/01/2018	Released

Accessibility

☒ PU, Public

☐ PP, Restricted to other program participants (including the Commission Services)

☐ RE, Restricted to other a group specified by the consortium (including the Commission Services)

☐ CO, Confidential, only for members of the consortium (including the Commission Services)

If restricted, please specify here the group:	

Owner / Main responsible:		
WP 6.2 Leader:	Berend Evenblij (TNO)	
Reviewed by:		
(WP 6 Leader:) (Technical Project Coordinator:) (Project Coordinator:)	Seppo Hänninen (VTT) Helfried Brunner (AIT) Luciano Martini (RSE))	20/12/2017
Final Approval by:		
ELECTRA Technical Committee TOQA appointed Reviewer:	Chris Caerts (VITO Helfried Brunner (AIT) Mihai Calin (IWES)	28/12/2017

Authors

Name	Last Name	Organization	Country
Berend	Evenblij	TNO	The Netherlands
Evangelos	Rikos	CRES	Greece
Kai	Heussen	DTU	Denmark
Junjie	Hu	DTU	Denmark
Michel	Rezkalla	DTU	Denmark
Mattia	Marinelli	DTU	Denmark
Atte	Löf	VTT	Finland
Riku	Pasonen	VTT	Finland
Seppo	Hänninen	VTT	Finland
Julia	Merino	TECNALIA	Spain
Emilio	Rodríguez	TECNALIA	Spain
Guillo Sansano	Efren	USTRATH	UK
Mazher	Syed	USTRATH	UK
Kevin	Johnstone	USTRATH	UK
Michal	Kosmecki	IEN	Poland

Copyright

Consisting of:

Coordinator	
Ricerca Sul Sistema Energetico – (RSE)	Italy
Participants	
Austrian Institute of Technology GmbH - (AIT)	Austria
Vlaamse Instelling Voor Technologisch Onderzoek N.V. - (VITO)	Belgium
Belgisch Laboratorium Van De Elektriciteitsindustrie - (LABORELEC)	Belgium
Danmarks Tekniske Universitet - (DTU)	Denmark
Teknologian Tutkimuskeskus - (VTT)	Finland
Commissariat A L'Energie Atomique Et Aux Energies Alternatives - (CEA)	France
Fraunhofer-Gesellschaft Zur Förderung Der Angewandten Forschung E.V – (IWES)	Germany
Centre For Renewable Energy Sources And Saving - (CRES)	Greece
Agenzia Nazionale per Le Nuove Tecnologie, L´Energia E Lo Sviluppo Economico Sostenibile - (ENEA)	Italy
Fizikalas Energetikas Instituts - (IPE)	Latvia
SINTEF Energi AS - (SINTEF)	Norway
Instytut Energetyki - (IEN)	Poland
Instituto De Engenharia De Sistemas E Computadores Do Porto - (INESC_P)	Portugal
Fundacion Tecnalia Research & Innovation - (TECNALIA)	Spain
Joint Research Centre European Commission - (JRC)	Belgium
Nederlandse Organisatie Voor Toegepast Natuurwetenschappelijk Onderzoek – (TNO)	Netherlands
Turkiiye Bilimsel Ve Teknolojik Arastirma Kurumu - (TUBITAK)	Turkey
University Of Strathclyde - (USTRATH)	UK
European Distributed Energy Resources Laboratories (DERlab)	Germany
Institute for Information Technology at University of Oldenburg (OFFIS)	Germany

Executive summary

In ELECTRA the future grid is seen as a Web-of-Cells. An ELECTRA Cell is a portion of the power grid able to maintain an agreed power exchange at its boundaries by using the internal flexibility of any type available from flexible generators/loads and/or storage systems. The total amount of internal flexibility in each cell shall be at least enough to compensate the cell generation and load uncertainties in normal operation. ELECTRA Cells can span multiple voltage levels, and connected to one or more neighbouring cells and can exchange power and data with them via one or more inter-cell physical tie-lines, and there is no restriction in how these inter-cell connections are organized: this can be radial or a mesh, or a combination of both.

Each Cell has a specific controller for each of the well-known grid-control aspects. These six controllers are as follows:

- Inertia control: Inertia Response Power Control (IRPC)
- Frequency control: Adaptive Frequency Containment Control (aFCC)
- Balance control:
    - Balance Restoration Control (BRC)
    - Balance Steering Control (BSC)
- Voltage control:
    - Primary Voltage Control (PVC)
    - Post-Primary Voltage Control (PPVC)

Each controller consists of an observing part (the observable algorithm) and a controlling part (the controller algorithm. The complete set of functions needed to build all the algorithms are described in present document. The aim of ELECTRA project is to develop those functions belonging to the higher control topology levels [1](CTL2 or CTL3), without neglecting completely CTL0 functions. The descriptions are done hand in hand with the coding of the functions in simulation software. The descriptions correspond therefore exactly to these simulation models. The developed codes are not included in the deliverable.

The implementation of Web-of-Cells control concept / use cases requires 11 specific core functions. This deliverable contains the descriptions of the following core functions categorised by controllers. Some of these functions are required by multiple controllers as follows:

- IPRC, aFCC and BRC: Merit Order Collection (MOC), Merit Order Decisions (MOD) and df/dt Droop Slope Determination function
- FCC: Adaptive Cell Power Frequency Characteristic function and Frequency Droop Parameter Determination function
- BRC: Imbalance Determination function and Imbalance Correction function
- BSC: Cell Set-point Adjusting function and Tie-line Limits Calculation function
- PPVC: The Post-Primary Voltage Controlling function and Post-Primary Voltage Set-point Providing function

The aforementioned core functions carry out following algorithms. The Merit Order Collection (MOC) function implements an algorithm that creates an activation-cost and size ordered list of available reserves, including location information. The Merit Order Decision function (MOD) filters this list to only retain resources that can be activated without causing local grid problems.

[1]A characteristic Topology Level at which a control loop operates. Here the following Control Topology Levels (CTLs) are used: CTL_0: Physical (single) Device Level; CTL_1: Flexible (aggregate) Resource Level; CTL_2: Cell level; CTL_3: Inter-cell level

Frequency Droop Parameter Determination function disaggregates the Cell Power Frequency Characteristic into droop factors of available reserves providing resources.

The Adaptive Cell Power Frequency Characteristic function scales these droop factors in relation to whether or not the cell is causing / contributing to an observed frequency deviation.

The Imbalance Determination function continuously observes the measured power over the tie-lines and the frequency for the determination of the power control error (PCE) in BRC use case. The cell control error (CCE) will determine the activation for the Imbalance correction function of BRC.

The Imbalance Correction function of the BRC use case determines the reserve activation control signals based on cell control error (CCE) value (depending on the type of resources) in order to correct the imbalance of the cell and the system frequency. The reserves list will determine the participation factor of each resource into the restoration process. The imbalance correction function developed combines fast acting devices along with conventional generation for an improved effectiveness of fast acting devices. It also allows for the activation of restoration reserves at the same time as containment reserves, improving the frequency response of the system.

The Cell Set-point Adjusting function is applied in BSC use case. It is aim is to adjust cell balance set-point taking into account tie-line limits, to decrease the number of reserves activations but without reducing the system balance restoration contributions. This provides a mitigation strategy for the fact that a distributed system balance restoration by means of cell balance restorations, loses the benefit of imbalance netting.

The Tie-line Limits Calculation function in BSC use case performs a simple calculation of the remaining available capacity of the tie-line to inform the Cell Set-point Adjuster functions of the capability of change in case of imbalance. The df/dt Droop Slope Determination function disaggregates the Cell Inertia contribution set-point into inertia providing set-points of contributing resources.

The Post-Primary Voltage Controlling function in PPVC use case has two different tasks assigned. Firstly, it checks the current voltage values in the nodes to determine, if they are within the regulatory safe band, and, if necessary, triggers the operation of the Post-Primary Voltage Set-point Providing function. Secondly, it communicates the voltage set-point values that are calculated by the Post-Primary Voltage Set-Point providing function to the available resources.

The Post-Primary Voltage Set-Point providing function determines the optimal voltage set-points in order to minimize power losses in the grid. It runs periodically, but each period can be pre-empted, if a voltage deviation is observed.

In addition of the core functions of controllers, the deliverable includes also descriptions of the following functions: Cell Inertia Set-point Provider, Rate of Change of Frequency Observer, Inertial Response Power Controller, Policy Calculation, PVC Controller, Grid Impedance Estimator. The Cell Inertia Set-point Provider function determines the inertia set-point to be respected on the synchronous area level and communicates to each cell their relative requested inertia set-point.

The Rate of Change of Frequency Observer function continuously samples voltage waveforms to calculate the local frequency and the rate of change of the frequency (ROCOF). This can be at either the connection point of a single device or a Point of Common Coupling of the aggregated resource.

The Inertia Response Power Controller increases or decreases active power generation or consumption in a manner proportional to the locally observed ROCOF. It has as input the ROCOF

(Δfloc/Δt) and the activation signal and as output the increased / decreased active power generation / consumption (continuously). The function bases on a proportional controller.

The Policy Calculation function works in the reserve scheduling phase, and the function will be used by the cell operator to make the reserve available. Two types of BRC regulation signals are considered here namely slow regulation signal and fast regulation signal. Two types of resource providers are assumed to be available in this cell, the slow generation units that mainly follow the slow regulation signal and the batteries that mainly follow the fast regulation signal. To allocate the basic schedule and reserves, a cost function for the slow generation unit and battery is defined.

The PVC Controller is a standard voltage droop controller.

The Grid Impedance Estimator (GIE) is a function of the PVC controller responsible for the current estimate of a value of the grid substitute impedance.

Aforementioned auxiliary functions are very important for the simulation of stand-alone and combinations of use cases and their lab validation.

Terminologies

Definitions

ELECTRA IRP developed definition and those from importance for the present document and the controllers area listed in table 1.

Table 1. Key definitions in the ELECTRA project

Term	Definition
Observable	A uniquely valued function of a number of measurable quantities in a physical system. An observable can be either a scalar or vector (“State Vector”) that is calculated from measured (observed) values in the present or past.
Observable algorithm	A detailed description of (or reference to) a specific set of operations that convert measurable values into an observable.
System Input Signal Time	A (scalar or vector) signal that is the input to the power system, in order to change the value of an observable. Time for system response or system control loops to complete the transition from a stationary system state to the next stationary state, after a switching event occurs within a power system.
Cell Balance Control	Control loops that control the cell balance which is defined as the aggregated power flow profiles over the tie-lines (i.e> import/export profiles).
Cell	An ELECTRA Cell is a portion of the power grid able to maintain an agreed power exchange at its boundaries by using the internal flexibility of any type available from flexible generators/loads and/or storage systems. The total amount of internal flexibility in each cell shall be at least enough to compensate the cell generation and load uncertainties in normal operation.

Abbreviations

ACE	Area Control Error
AGC	Automatic Generation Control
aFCC	Adaptive Frequency Containment Control
BRC	Balance Restoration Control
BSC	Balance Steering Control
CCE	Cell Control Error
CPFCCTL	Cell Power Frequency Characteristic Control Topology Levels
CSACPFC	Cell Set-point Adjusting Cell Power Frequency Characteristic
CTLCSA	Control Topology Level Cell Set-point Adjusting
CTL-0	Control Topology Level 0: Physical (single) Device Level
CTL-1	Control Topology Level 1: Flexible (aggregate) Resource Level
CTL-2	Control Topology Level 2: Cell level
CTL-3	Control Topology Level 3: Inter-cell level
CTS	Control Time Scales
DERCTS	Distributed Energy Resources Control Time Scales
DDSDDER	Df/dt Droop Slope Determination, Distributed Energy Resources
FCCDDSD	Frequency Containment Control Df/dt Droop Slope Determination,
FDPDFCC	Frequency Droop Parameter Determination Frequency Containment Control
GIEFDPD	Grid Impedance Estimator Frequency Droop Parameter Determination
HLUCGIE	High Level Use Case Grid Impedance Estimator
ICHLUC	Imbalance Correction High Level Use Case
IMOIC	Initial Merit Order Imbalance Correction
IPMIMO	Interior Point Method Initial Merit Order
IRPIPM	Integrated Research Program Interior Point Method
IRPCIRP	Inertia Response Power Control Integrated Research Program
MOCIRPC	Merit Order Collection Inertia Response Power Control
MOLMOC	Merit Order List Merit Order Collection
NPFCMOL	Network Power Frequency Characteristic Merit Order List
OPFNPFC	Optimal Power Flow (OPF)Network Power Frequency Characteristic
PCCOPF	Point of Common Coupling Optimal Power Flow (OPF)
PCEPCC	Power Control Error Point of Common Coupling
PIPCE	Proportional Integral Power Control Error
PJM Reg A and Reg DPI	PJM is trademark and Reg A and Reg D are types of regulation Proportional Integral
PLLPJM Reg A and Reg D	Phase Lock Loop PJM is trademark and Reg A and Reg D are types of regulation
PMUPLL	Phasor Measurement Unit Phase Lock Loop
PPVCPMU	Post-Primary Voltage Control Phasor Measurement Unit
PVPPVC	Photo Voltage Post-Primary Voltage Control
PVCPV	Primary Voltage Control Photo Voltage
RESPVC	Renewable Energy Sources Primary Voltage Control
ROCOFRES	Rate of Change of the Frequency Renewable Energy Sources
UCSGAMROCOF	Use Case Smart Grid Architecture Model Rate of Change of the Frequency
SRPSSGAM	Single Reference Power System Smart Grid Architecture Model
UCSRPS	Use Case Single Reference Power System
VPPUC	Virtual power plants Use Case
VPP	Virtual power plants

Table of contents

List of figures and tables

1. Introduction

This deliverable presents the detailed descriptions (later also called “White-box-descriptions”) of the core and main auxiliary functions for the functional architecture of the ELECTRA Web-of-Cells control scheme Use Cases. The ELECTRA Web-of-Cells concept is a proposed decentralized control scheme for the real-time frequency/balance and voltage control of the future grid. The development procedure of the control functions bases on the descriptions of the use cases which can be found in the Electra Deliverable D4.2 [4]. This deliverable elaborates the preliminary function descriptions into “White-box” descriptions that capture detailed design decisions and implementation choices and details as part of the implementation and testing and validation activity.

In order to maintain frequency (balance) and voltage control in the future power system, the ELECTRA Web-of-Cells control scheme introduces six high-level use cases, which are

- Inertia control: Inertia Response Power Control (IRPC)
- Frequency control: Adaptive Frequency Containment Control (aFCC)
- Balance control:
  - Balance Restoration Control (BRC)
  - Balance Steering Control (BSC)
- Voltage control:
  - Primary Voltage Control (PVC)
  - Post-Primary Voltage Control (PPVC)

Within ELECTRA, the functions and interactions are kept as simple as possible in view of what is needed to test and validate the control scheme (lab-scale proof of concept functional validation). A number of functions that would be required for a real world implementation and deployment (like an aggregation of reserves) is left out (though its impact related to additional latencies in information exchanges are modelled in a way to be parametrised). Concerning the functions providing the observables (like the frequency or the tie-line power flow deviation error signal) or that actuate the control signal (like droop behaviour), a distinction is made between those for which a novel approach has been developed in the project, and those for which standard existing technology (and libraries in the simulation environment) can be used. Besides, other functions that are needed for the simulation and testing, but are not the focus of the control scheme itself, like the forecasting of load and generation profiles, or the determining of the availability profile and cost of reserves, are modelled and abstracted by means of a database or file read implementation. The development of the white-box starts from the preliminary descriptions and is an iterative implementation process containing “white-boxing”, coding and simulation. White-box descriptions contain among others the detailed specifications of the operation principles, possible block diagrams of the control implementation, algorithms, mathematical equations, as well as decomposition of black-box functions into finer granularity functionality.

The ELECTRA Use Case description forms the starting point of the activities leading to this document [4]:

1. Making white box descriptions of each function.
2. Implementing each function in code in order to be implemented in a simulation and lab-testing environment. The codes are not included in this deliverable.
3. Evaluation by a simple simulation that the code is sufficiently bug-free and functional.
4. Evaluation by simulation in one of the two selected test-grids that each use case is functional in stand-alone mode. This part of the work is presented in Electra D6.4.

The present document contains the white box descriptions of the functions in order to enable the ELECTRA WoC Use Cases including Observable Algorithms and Controller Algorithms, see Fig. 1.

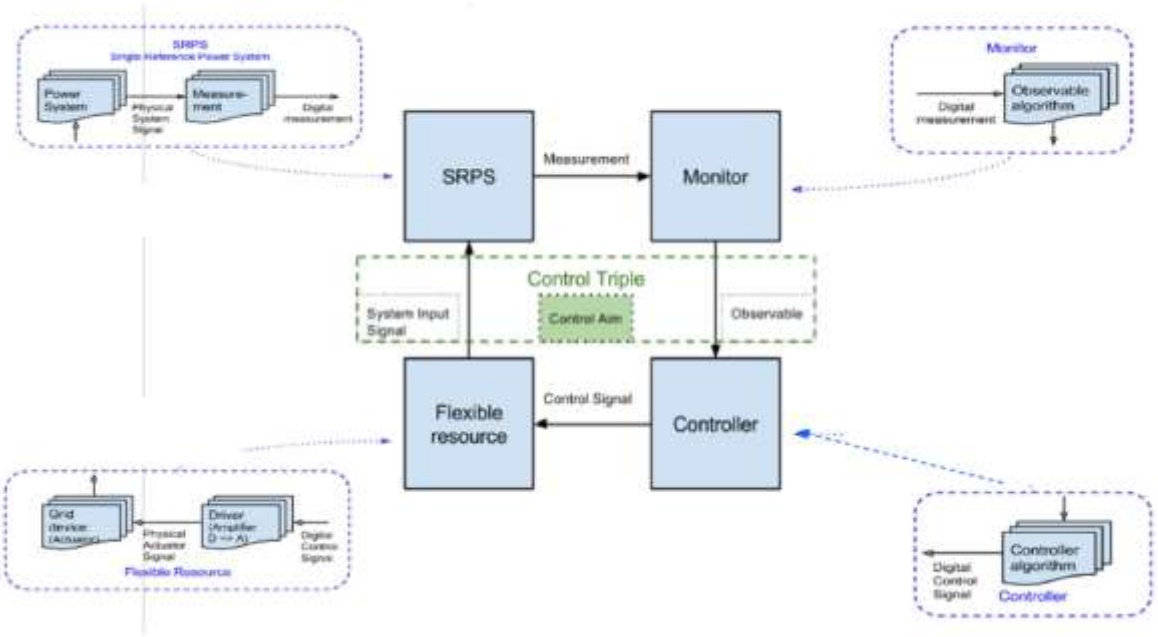

Figure 1. Relation to the control triple structure [5]

The Observable Algorithm is a specific set of operations that convert measurable values into an observable. It corresponds to the upper right blue square “Monitor”. The monitor includes the Observable Algorithms and its interfaces.

The Controller Algorithm transforms the observable into a control signal (See the lower right blue square “Controller”. The Figure 2 shows an overview of the use cases and the related function.

The white box descriptions presented in this document are those that are defined as ELECTRA in-scope functions for the complete set of the Use Cases. They can be seen as representing the core functionality. They are described in chapter 2.

Beside these in-scope functions there are needed some essential auxiliary functions to facilitate a working system. These are described in chapter 3.

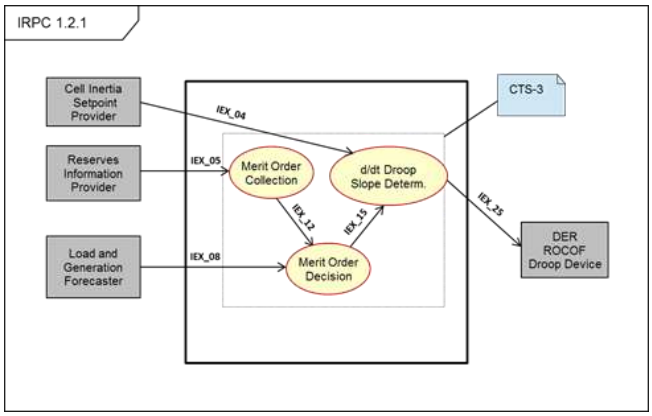

Inertia Response Power Control

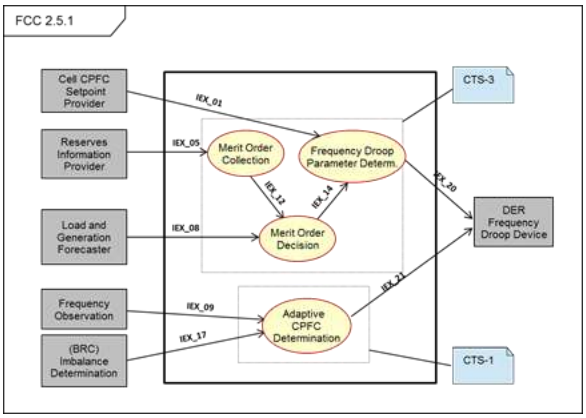

Frequency Containment control

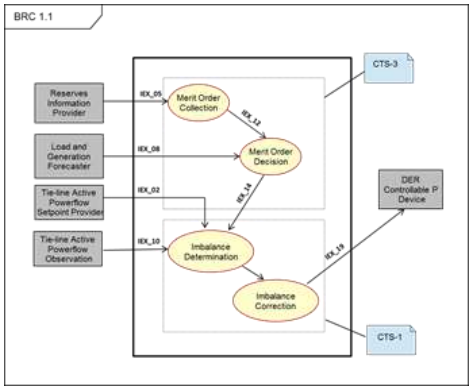

Balance restoration Control

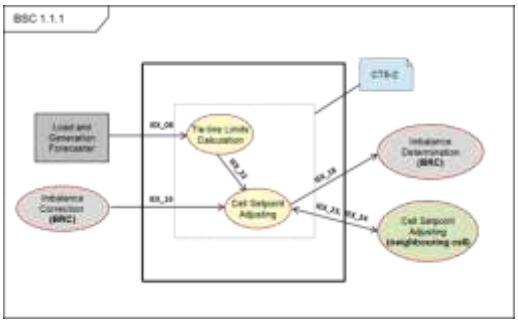

Balance Steering Control

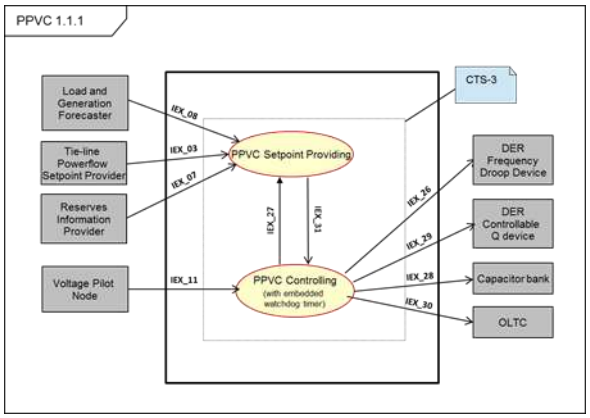

Post Primary Voltage Control

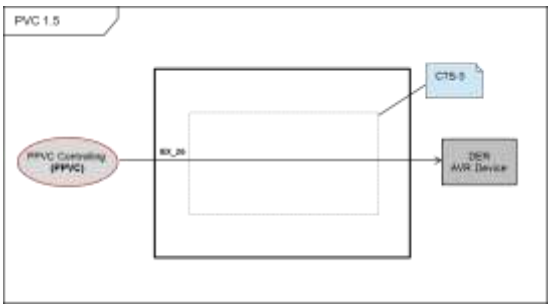

Primary Voltage Control

Figure 2. The overview of the Use Case and the related functions [4]

2. White box descriptions of in scope functions

2.1. Merit Order Collection

The Merit Order Collection (MOC) function implements an algorithm in order to collect all available reserves' status. It collates them in a list initially ranked based on the European Article Number (EAN, a unique identity number for each unit; for our purpose uniquely defining and localizing the connected resource) of each reserve and, next sort twice the list based first and foremost on cost/W (ascending order with cheapest reserves first) and then based on the size of the reserve, see Fig. 3.

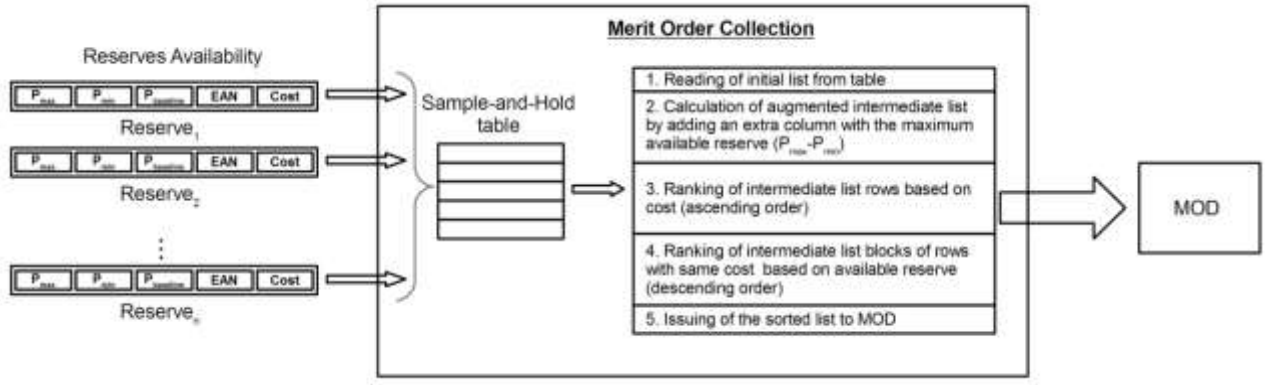

Figure 3. Block diagram of the Merit Order Collection control implementation

The detailed procedure that the merit order collection (MOC) follows is described below:

1. At first, the function reads the value of each reserve's availability. The value is a vector containing the following quantities: P_{max}, P_{min}, $P_{baseline}$, EAN and cost/Watt. In our approach, $P_{baseline}$ represents the forecast or scheduled power that a resource is expected to deliver or consume in the next time frame or, in other words, the power of the reserve if no activation is requested. For example, for a PV this parameter can only be a forecast value whereas the power of a battery storage system can be the scheduled one. Likewise, P_{min} and P_{max} indicate the maximum range of power variation of the resource in relation to its $P_{baseline}$, its operating limits and any other possible constraint. In principle, the information of reserves' availability must be an array of many such vectors. We assume that within each timestep (e.g. 15-min) these are constant values, although of course in reality, this could be profiles (in which case the reserves's availability would be expressed as a vector of vectors, where for each finer granularity timestep – e.g. 1-min – the P_{max}, P_{min}, $P_{baseline}$, EAN and cost/Watt must be given.
2. Since the values of step1 are issued by each reserve they may arrive asynchronously. Therefore, the EAN value is used as trigger signal and as long as this is non-zero the vector is sampled and held in a 5xn matrix (5 rows representing the abovementioned quantities and n columns for n reserves). Each column corresponds to a respective EAN.
3. The above matrix is transposed and used as the initial list.
4. The initial list is augmented with an extra column representing the maximum capacity of each reserve, namely P_{max}-P_{min}.
5. The intermediate list is sorted based on ascending cost.
6. The blocks of rows with the same cost are sorted based on descending capacity based on the added column.

7. After sorting is completed, the final list is derived as the reduced intermediate list, excluding the extra column of step 5 as well as the cost column (column 5).
8. The final list is issued to the Merit Order Decision function, see Fig. 4.

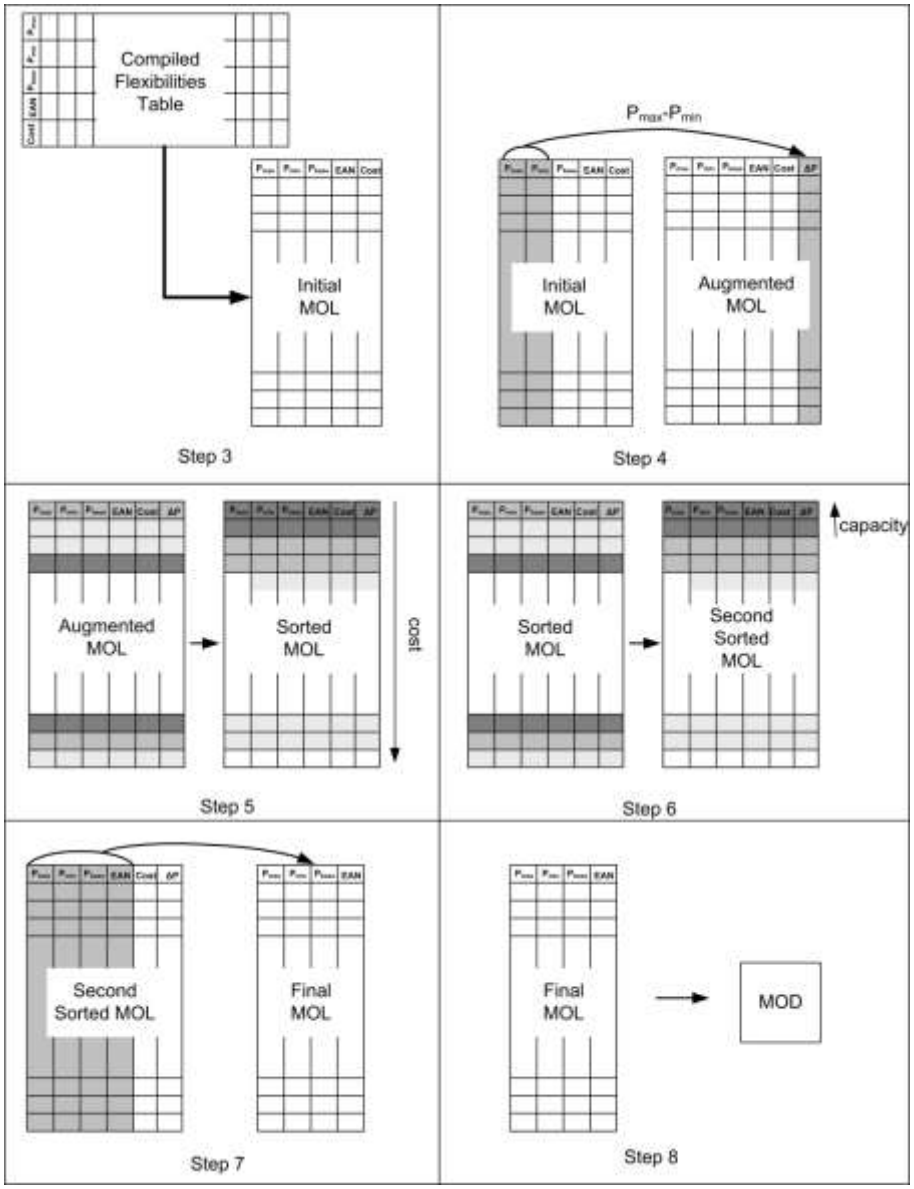

Figure 4. Simplified illustration of steps 3 to 8 in the Merit Order Collection function

2.2. Merit Order Decision

The Merit Order Decision (MOD) function (see Fig. 5) uses the initial merit order list produced by the Merit Order Collection function in order to refine it by selecting only the reserves that have no negative impact on the grid i.e. whose activation would not cause a local grid problem. The function includes a load flow analysis, in which it calculates the voltages of all buses, under the assumption of a steady state with the reserves activated to their worst grid impacting value, i.e. they can reach either their P_{max} or their P_{min} since both are the worst case scenarios in terms of reserves activation. Apparently, voltages or congestion problems can be caused by any intermediate state of the reserves too. In this analysis, for the sake of simplicity we assume only the extreme case of full activation. If some of the nodes' voltages are above or below a maximum

allowable limit or the line currents exceed the maximum capacity of the line, the reserves at the relevant bus are excluded. Ideally, in such a case the algorithm should investigate a lower activation power for the specific reserves, but due to the increased complexity of this algorithm only for the implementation of the specific function we have considered the extreme case of excluding a reserve once a problem at its maximum activation is detected.

The implementation of this algorithm requires the detailed power schedules of all resources (generation, loads and storage units) and not only the ones used as reserves. This power schedule contains the same $P_{baseline}$ power considered in the MOC function in conjunction with the EAN for the corresponding unit. In addition, it contains the reactive power schedule of the units. The form of this power schedule is again an array with as many rows as all the resources connected to the cell and corresponds to the next timeframe of 15 min. The values of all timeframes can be stored in the same 2D array in multiple row blocks each one corresponding to one timeframe.

In addition, this function has information regarding connectivity of resources (i.e. which bus each resource is connected to) in the form of a constant array that contains rows with the EAN of each resource, the bus (node) to which it is connected, as well as the type of bus. Also, it has information regarding the grid topology (line impedances, and interconnections among buses) in the form of a constant matrix.

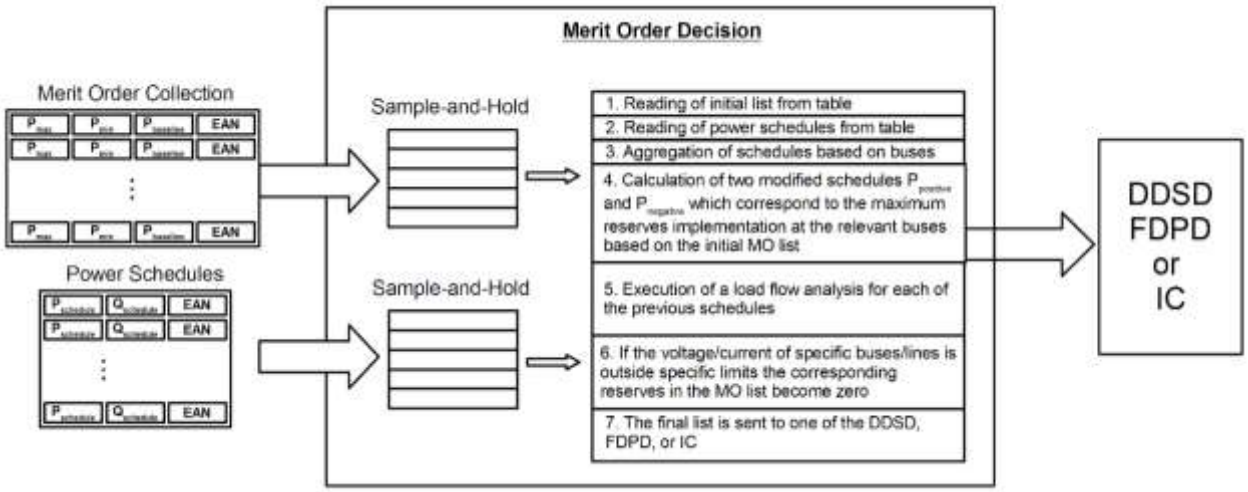

Figure 5. Block diagram of the Merit Order Decision control implementation

The detailed procedure that MOD follows is the following:

1. First, the function reads the initial Merit Order List provided by the MOC. This list consists of rows containing the following information: P_{max}, P_{min}, $P_{baseline}$ and EAN.
2. The function requests and gets the detailed power schedules for all resources for the next time window. The array contains rows with three values, namely $P_{scheduled}$, $Q_{scheduled}$ and EAN
3. For the load flow implementation the individual power values are aggregated at bus level so that at the end each bus has one pair of P and Q values. In order to do so, the function uses connectivity data in the form of a table that contain three columns: EAN, bus number and bus type.
4. Once the aggregated schedules are obtained, two separate active power schedule modifications are derived by modifying the initial aggregate schedule by the maximum positive/negative reserves on the relevant buses. For this, the Initial Merit Order (IMO) is used. The values of the list are associated to the buses by means of EAN and the number

of the corresponding bus from the grid connectivity data from step 3.

5. For each separate schedule (positive and negative) a load flow calculation is performed. For instance, a large, positive frequency deviation which implies a surplus in production requires a high negative power deviation in the cell. Eventually, the function performs the load flow analysis and calculates the voltages of all buses and current flows in all lines. The details of the load flow algorithm implemented are described below:
    a. The matrix Y_{bus} of the grid admittances is calculated based on a stored data table that contains the following rows: Line number, starting bus number, ending bus number, impedance (pu) and admittance (pu).
    b. The vectors of voltage magnitudes and angles are initialised appropriately.
    c. Initial deviations for active and reactive powers for each bus are calculated using the equations.

$$P_i = P_{Gi} - P_{Li} = \sum_{j=1}^{n} |V_i||V_j||y_{ij}|cos(\delta_j - \delta_i + \gamma_{ij}) \quad (1)$$

$$Q_i = Q_{Gi} - Q_{Li} = -\sum_{j=1}^{n} |V_i||V_j||y_{ij}|sin(\delta_j - \delta_i + \gamma_{ij}) \quad (2)$$

    d. All elements of the augmented Jacobian matrix are calculated (first partial derivatives active/reactive powers over state variables |V| and δ using the formulas:

Matrix H

$$(\frac{\partial P_i}{\partial \delta_j})^{(k)} = -|V_i^{(k)}||V_j^{(k)}||y_{ij}|sin(\delta_j^{(k)} - \delta_i^{(k)} + \gamma_{ij}) \quad (3)$$

$$(\frac{\partial P_i}{\partial \delta_i})_i^{(k)} = \sum_{j=1, j\neq i}^{n} |V_i^{(k)}||V_j^{(k)}||y_{ij}|sin(\delta_j^{(k)} - \delta_i^{(k)} + \gamma_{ij}) \quad (4)$$

Matrix N

$$(\frac{\partial P_i}{\partial |V_j|})_i^{(k)} = |V_i^{(k)}||y_{ij}|cos(\delta_j^{(k)} - \delta_i^{(k)} + \gamma_{ij}) \quad (5)$$

$$(\frac{\partial P_i}{\partial |V_i|})_i^{(k)} = 2|V_i^{(k)}||y_{ii}|cos\,(\gamma_{ii}) + \sum_{j=1, j\neq i}^{n} |V_j^{(k)}||y_{ij}|cos(\delta_j^{(k)} - \delta_i^{(k)} + \gamma_{ij}) \quad (6)$$

Matrix M

$$(\frac{\partial Q_i}{\partial \delta_j})_i^{(k)} = -|V_i^{(k)}||V_j^{(k)}||y_{ij}|cos(\delta_j^{(k)} - \delta_i^{(k)} + \gamma_{ij}) \quad (7)$$

$$(\frac{\partial Q_i}{\partial \delta_i})^{(k)} = \sum_{j=1, j\neq i}^{n} |V_i^{(k)}||V_j^{(k)}||y_{ij}|cos(\delta_j^{(k)} - \delta_i^{(k)} + \gamma_{ij}) \quad (8)$$

Matrix L

$$(\frac{\partial Q_i}{\partial |V_j|})_i^{(k)} = -|V_i^{(k)}||y_{ij}|sin(\delta_j^{(k)} - \delta_i^{(k)} + \gamma_{ij}) \quad (9)$$

$$\left(\frac{\partial P_i}{\partial |V_i|}\right)_i^{(k)} = -2|V_i^{(k)}||y_{ii}|sin\,(\gamma_{ii}) - \sum_{j=1, j\neq i}^{n} |V_j^{(k)}||y_{ij}|sin(\delta_j^{(k)} - \delta_i^{(k)} + \gamma_{ij}) \quad (10)$$

e. Based on the bus type, the relevant Jacobian elements as well as equations are omitted from the solutions (i.e. slack, PV buses).
f. The final Jacobian matrix is inversed and used to produce the new improved |V| and δ vector of values. The algorithm implemented is the Newton-Raphson method

$$\begin{bmatrix} \underline{\delta}^{(k+1)} \\ \underline{|V|}^{(k+1)} \end{bmatrix} = \begin{bmatrix} \underline{\delta}^{(k)} \\ \underline{|V|}^{(k)} \end{bmatrix} + \left(\begin{bmatrix} H^{(k)} & N^{(k)} \\ M^{(k)} & L^{(k)} \end{bmatrix}\right)^{-1} \cdot \begin{bmatrix} \underline{\Delta P}^{(k)} \\ \underline{\Delta Q}^{(k)} \end{bmatrix} \quad (11)$$

g. The improved values are used to recalculate the deviations in step c
h. Steps c to g are repeated for 15 iterations maximum

6. Once the vector of voltage magnitudes is obtained, these values are compared with a threshold value for positive/negative activation.
7. If, for instance, a voltage is above (below) the selected limit the reserves capacities of all resources connected to the specific bus become zero (i.e. the maximum/minimum power in the IMO becomes equal to the actual power).
8. The final list is sent to the concerned IRPC, FCC, and BRC functions, namely df/dt Droop Slope Determination (DDSD-see chapter 2.9), Frequency Droop Parameter Determination (FDPD, see chapter 2.3) and Imbalance Correction (IC- see chapter 2.6).

2.3. Frequency Droop Parameter Determination

The proposed control function implements a strategy in order to divide all available FCC reserves into frequency in order to avoid the simultaneous activation of all reserves in a frequency deviation, but to obtain a scalable activation through frequency deadband values for each reserve. This way, the cheapest reserves can be used first for the very small and more frequent imbalances, and if these deviations exceed specific limits more and more reserves are activated. More analytically, the Frequency Droop Parameter Determination (FDPD) receives two input signals, namely one Cell Power-Frequency Characteristic (CPFC) value that is used as a set-point and a table of values (as a second input) which corresponds to the final (optimised) Merit Order list of all acceptable reserves (see Fig. 6). The output of this procedure is another table containing droop slopes as well as frequency values (activation thresholds or deadbands) for the selected FCC reserves. Based on whether a slope for a Distributed Energy Resources (DER) is non-zero or not, it decides if it has to communicate the corresponding signal to the corresponding DER.

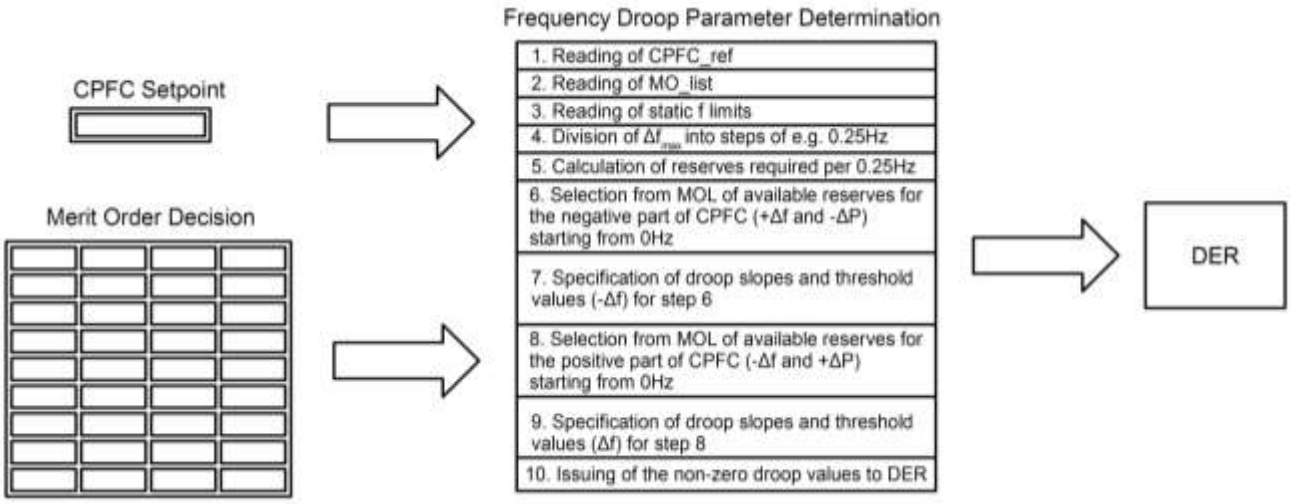

Figure 6. Block diagram of the Frequency Droop Parameter Determination control implementation

The detailed procedure that FDPD follows is described below:

1. At first, the function reads the values of CPFC set-point (in W/Hz). For the sake of convenience in the internal calculations this value is negated so that the positive value of it is eventually used.
2. In addition, FDPD reads the Merit Order list, which is a table containing three power values (P_{max}, P_{min} and $P_{baseline}$) together with the identity value (EAN) of the resource that provides the reserve. The order indicates the priority of reserves use that FDPD should follow, and the three power values are used by FDPD in order to specify which reserves can respond to positive or negative power frequency changes by offering power decrease, increase or both (see Fig. 7).
3. Once the inputs are read, FDPD reads the static limits of frequency deviations (e.g.±1Hz) and calculates the frequency threshold steps by dividing the former margins to 4(8) steps. The goal of this division is to produce steps of indicatively 0.25Hz.
4. For each frequency step and based on the CPFC set-point FDPD calculates the amount of required power (e.g. 160000W/Hz correspond to 40000W if 0.25Hz steps are selected).
5. For the negative part of the CPFC, FDPD starts scanning the MO list from top to bottom. If a reserve can decrease its power (i.e. $P_{baseline}>P_{min}$), the total power of this reserve is added.
6. The sum is compared with the power requirement from step 4. If it is lower than that, it proceeds to the next reserve. The slope of each selected reserve is set to ($P_{baseline}$-P_{min})/0.25Hz of the specific reserve, and its negative threshold is set to 0Hz. If a reserve from the list cannot decrease power, its slope is simply set to 0. These values are stored in matrix (in columns 1 and 3 respectively).
7. When by adding the last reserve the sum exceeds the power requirement, only the power difference is used by the last added reserve and its slope is calculated as ($P_{requirement}$-P_{sum})/0.25Hz.
8. At this point the first frequency slot (0, -0.25Hz) has been fully covered. The steps 5-7 are repeated for the next frequency slots, namely (-0.25Hz, -0.5Hz), (-0.5Hz, -0.75Hz) etc., until the minimum allowable frequency deviation is reached (e.g. slot (-0.75Hz, -1Hz).
9. For the positive part of CPFC, FDPD follows a similar procedure looking at reserves that can increase their power (i.e. $P_{max}>P_{baseline}$). Again, the MO list is scanned from top to bottom repeating essentially steps 5-7, but this time the slopes are (P_{max}-$P_{baseline}$)/0.25Hz.

This value (or zero slope for the reserves that cannot increase power) is stored in the output matrix in column 2 together with the corresponding positive threshold (column 4).

10. Finally, the FDPD assigns all corresponding EANs to the fifth column of the matrix for association of the selected parameters to the corresponding DER units.

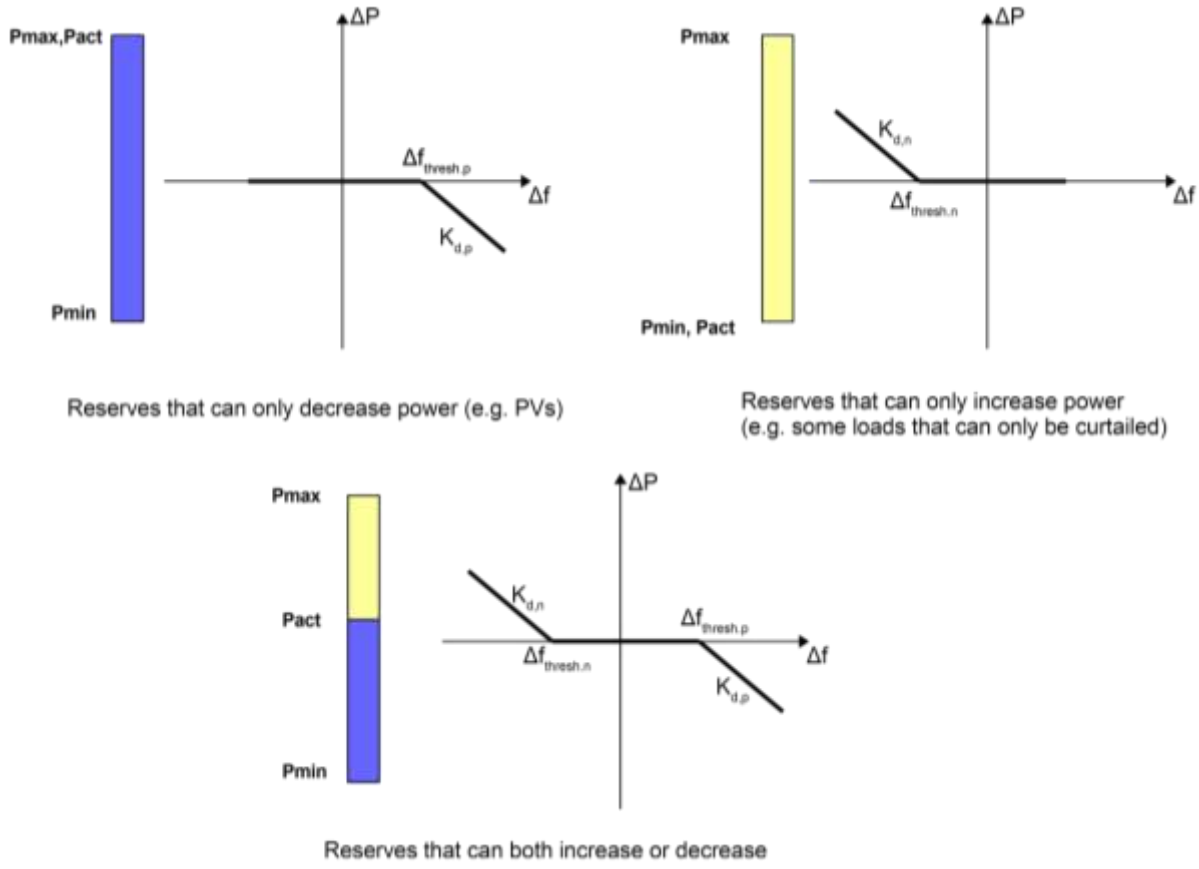

Figure 7. Various types of reserves with respect to the power flow direction capabilities

Figure 8 summarizes the above procedure in the form of a flow chart.

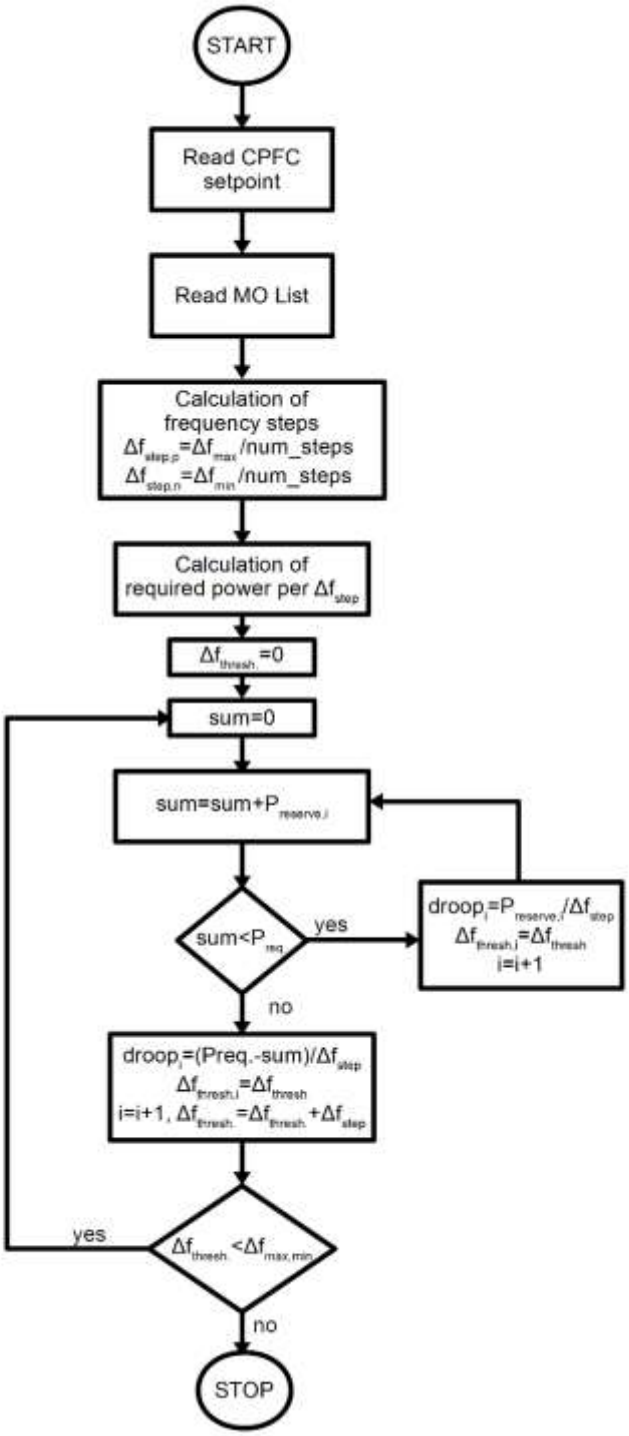

Figure 8. Flowchart illustrating the Frequency Droop Parameter Determination procedure

2.4. Adaptive Cell Power Frequency Characteristic Determination

The proposed adaptive determination of Cell Power Frequency Characteristic control function (CPFC) uses fuzzy logic and is briefly described in Fig. 9. In this diagram, a cell's frequency response to imbalances is represented by the transfer function $G_{p1}(s)$, and it involves the parameters of inertia constant H as well as load self-regulation in the following relationships:

$$K_{pi} = \frac{1}{D_i}, T_{pi} = \frac{2H_i}{f^0 D_i} \quad (12)$$

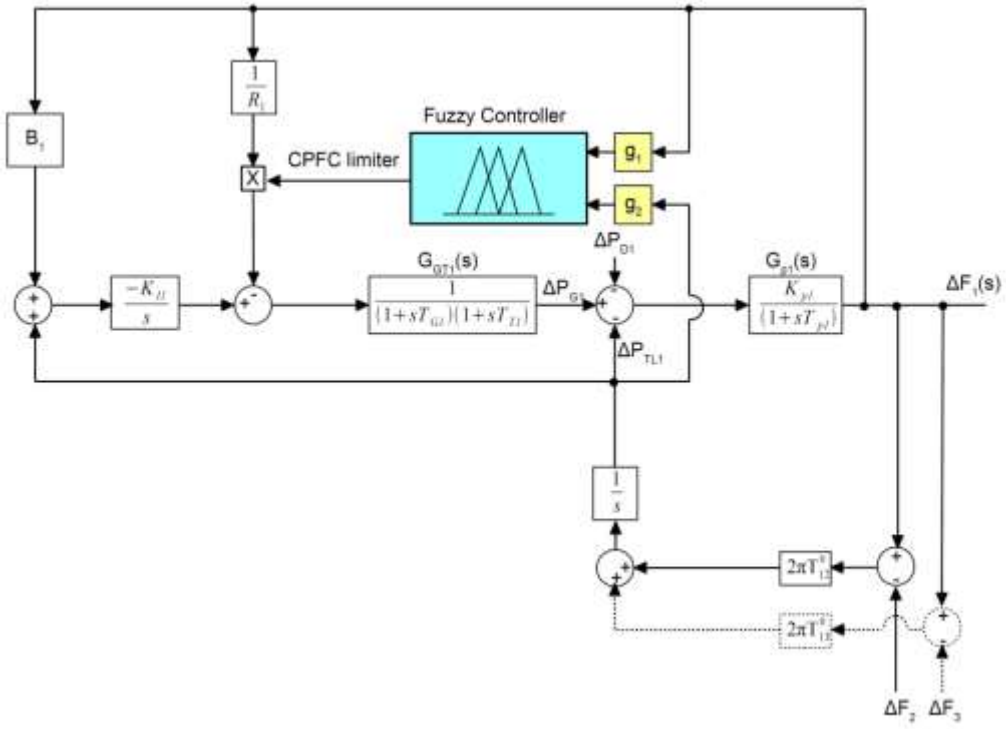

Figure 9. Block diagram of the Adaptive Cell Power Frequency Characteristic Determination control implementation

Table 2 provides an overview of this model's main parameters.

Table 2. System Parameters for the Cell Power Frequency Characteristic model

Symbol	Description
H_i	Inertia constant in [sec]
D_i	Load self-regulation in [puMW/Hz]
K_{pi}	Area's constant in [Hz/puMW]
T_{pi}	Area's time constant [sec]
T_{ij}	Tie-line static limit [puMW/rad]
R_i	Droop slope in [Hz/puMW]
B_i	Frequency bias [puMW/Hz]
T_{Gi}	Governor's time constant in [sec]
T_{Ti}	Turbine's time constant in [sec]
K_{Ii}	Integrator's gain

The adaptive control in this case is obtained by means of a fuzzy logic controller receiving frequency and tie-line power deviations as input signals and derives a factor, which is used as a scaling ratio for the full-scale droop control of the cell. Specifically, the controller uses the combination of both Δf_i and $\Delta P_{tie,i}$ in order to identify the cell's state, where:

$$\Delta P_{Tie,i} = \sum_{j=1}^{m} \Delta P_{Tie,ij} \quad (13)$$

The premise of this approach is when an imbalance incident happens in one cell, the frequency initially increases/decreases based on the imbalance sign and, by the same token, the tie-line error aggregate follows an opposite, to the frequency course. Thus, by detecting the combined signs as well as sizes of the two errors, it is possible to adjust the droop slope of the cell when the incident takes place outside the cell or maintain its maximum value whenever the incident concerns the specific cell. The membership functions of the selected controller are depicted in Fig. 10. As it is shown in this diagram and in Table 3, we have used some linguistic variables to describe the membership function of the input variables as follows: (Negative High-NH, Negative Low-NL, Zero-ZE, Positive Low-PL, and Positive High-PH). In this implementation, the input and output signals consist of triangular functions. The maximum frequency range is from 48 to 52Hz (±2Hz) and the maximum tie-line error varies from -1 to +1 puMW. However, these limits are easily modifiable by means of two gains in the input signals, namely gains g_1 and g_2. In any case, the output, namely $CPFC_r$, consists of four membership functions, which produce a gradual reduction from 100 to 0%.

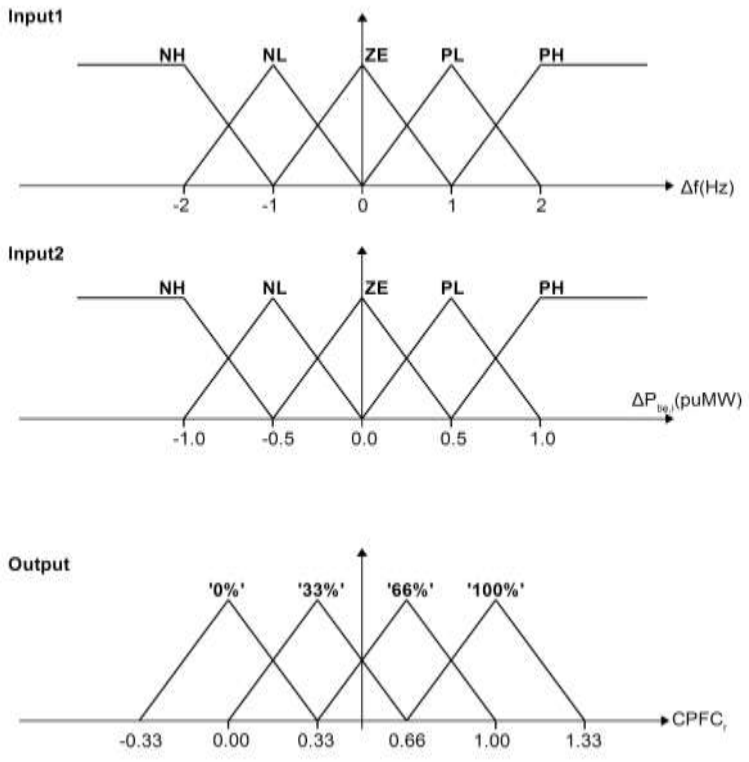

Figure 10. Fuzzy membership functions for one implementation example of the Adaptive Cell Power Frequency Characteristic Determination

The rules used for the proposed adaptive control are summarised in the rule table (Table 3). As it can be seen in these tables, the occurrence of error signals with opposite signs entails incidents inside the cell, thus the CPFC coefficient remains unchanged. By contrast, there is a reduction in the CPFC value whenever the signs of the errors are the same, with a specific reduction selection

based on the size of the error. For example, in table 3 a combination of input signals such as Δf=-1Hz and $\Delta P_{tie,i}$=-0.5puMW ($g_1=g_2=1$) yields a $CPFC_r$=66%.

Table 3. Rule table for the adaptive Cell Power Frequency Characteristic Determination

$\Delta P_{tie,i}$ / Δf	NH	NL	ZE	PL	PH
NH	0%	33%	100%	100%	100%
NL	33%	66%	100%	100%	100%
ZE	66%	100%	100%	100%	66%
PL	100%	100%	100%	66%	33%
PH	100%	100%	100%	33%	0%

The calculation of the crisp output value is obtained by means of the Centre-of-Gravity method, which takes into account the chopped membership functions of the input signals:

$$CPFC_{coef.}{}^{crisp} = \frac{\sum_i b_i \int \mu_{(i)}}{\sum_i \int \mu_{(i)}} \tag{14}$$

Where, b_i is the centre-of-gravity point of the output membership function $\mu_{(i)}$. In our case the corresponding points are: b_i={0.00, 0.33, 0.66, 1.00}.

Example:

For a set of input values Δf=-0.25Hz and $\Delta P_{tie,i}$=0.25puMW the membership functions of the input signals are shown in Fig.10. Based on Table 2 the rules that are satisfied for these inputs are four:

IF Δf is 'NL' **and** $\Delta P_{tie,i}$ is 'PL' **THEN** $CPFC_r$ is '100%'

IF Δf is 'NL' **and** $\Delta P_{tie,i}$ is 'ZE' **THEN** $CPFC_r$ is '100%'

IF Δf is 'ZE' **and** $\Delta P_{tie,i}$is 'PL' **THEN** $CPFC_r$ is '100%'

IF Δf is 'ZE' **and** $\Delta P_{tie,i}$ is 'ZE' **THEN** $CPFC_r$ is '100%'

The corresponding $\mu_{(i)}$ values are selected as follows:

$$\mu_{(i)} = min\{\mu(\Delta f), \mu(\Delta P_{tie,i})\} \tag{15}$$

Which yields:

$\mu_{(12)}$=min(0.25, 0.5), $\mu_{(13)}$=min(0.25, 0.5), $\mu_{(17)}$=min(0.75, 0.5) and $\mu_{(18)}$=min(0.75, 0.5)

Finally, by using the following formula for the calculation of the area of each $\mu_{(i)}$ (see fig. 11) namely:

$$\int \mu_{(i)} = w_i \cdot \left(h_i - \frac{h_i^2}{2}\right) \tag{16}$$

Where w and h are explained in Fig. 12. Finally, the crisp value of the output based on (3) is:

$$CPFC_{coef.}{}^{crisp} = \frac{0.144375 \cdot 1 + 0.144375 \cdot 1 + 0.309375 \cdot 1 + 0.309375 \cdot 1}{0.144375 + 0.144375 + 0.309375 + 0.309375} = 1$$

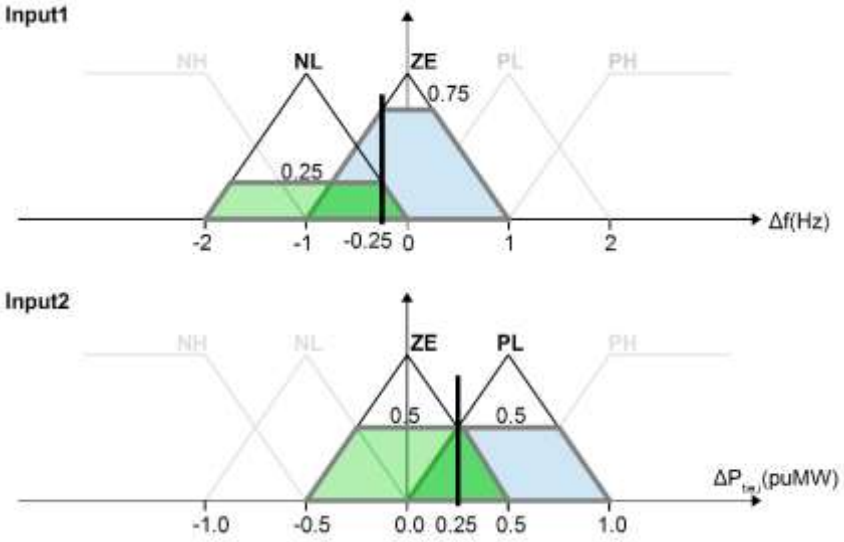

Figure 11. CPFC Determination membership functions for inputs Δf=-0.25Hz and $\Delta P_{tie,i}$=0.25puMW

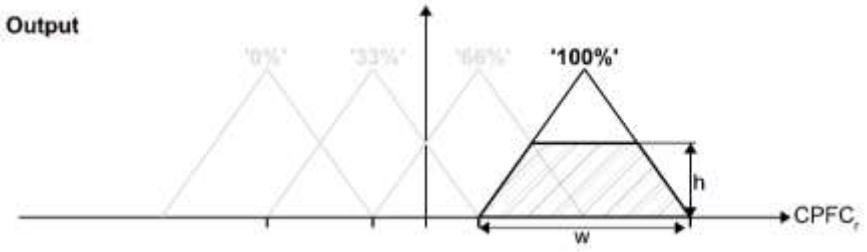

Figure 12. Calculation of each $\mu_{(i)}$ area

2.5. Imbalance Determination

This function continuously observes the measured power over the tie-lines and the frequency for the determination of the power control error (PCE) and the cell control error (CCE). The PCE and CCE will determine the activation and set points for the Imbalance correction function of BRC.

The Cell Control Error (CCE) is implemented in a similar manner to current ENTSO-E Area Control Error (ACE) measurement.

$$CCE_i = \left(\sum_{j=1}^{n} P_j^{TLsched} - \sum_{j=1}^{n} P_j^{TLmeas} \right) + \beta_i (f_0 - f_{meas}) \quad (17)$$

$$\beta_i = (1/R)D \quad (18)$$

Where, CCE_i is the CCE of cell i, n is the number of tie-lines from the cell i to other cells, $P_j^{TLsched}$ is the scheduled net interchange over tie-line j, P_j^{TLmeas} is the measured net interchange over tie-line j, f_0 is the nominal frequency (50Hz for European Grid), f_{meas} is the measured frequency. β_i is

the bias factor that it is usually defined based on experience and equivalent to Equation 18, where, R is the representative droop of the cell and D is the load damping characteristic.

The CCE can be divided into two components, a power components and a frequency component, the power component describes the total power flow error of the cell by comparing measured and scheduled power flows of the cell tie-lines.

$$PCE_i = \left(\sum_{j=1}^{n} P_j^{TLsched} - \sum_{j=1}^{n} P_j^{TLmeas} \right) \tag{19}$$

Along with these determined imbalances, this function determines whether the imbalance has been produced within the cell or at an external cell. This will allow for solving local problems with local resources. This is performed by means of the algorithm shown in the flowchart of Fig.13.

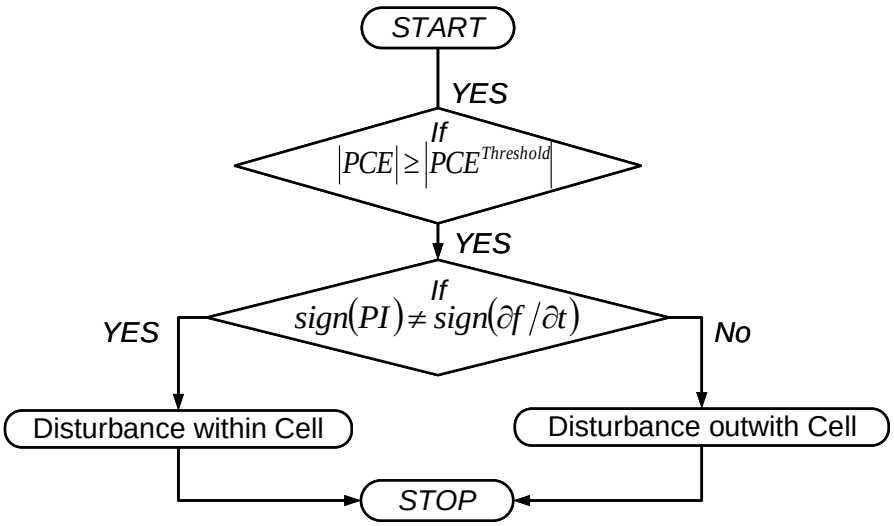

Figure 13. Disturbance detection algorithm for Imbalance Determination

The first condition of the algorithm confirms that a deviation in PCE exists and it is beyond a set threshold as:

$$|PCE| \geq |PCE^{Threshold}| \tag{20}$$

The restoration control is designed not to operate for deviations in PCE within the set threshold. The satisfaction of this condition confirms the occurrence of a significant event within the network, however, it is the second condition that establishes whether the disturbance is within cell or not, and can be represented as:

$$sign\,(PCE) \neq sign\left(\frac{\partial f_{meas}}{\partial t}\right) \tag{21}$$

where, $\partial f_{meas}/\partial t$ is the rate of change of frequency.

When these two conditions are met a TRUE location value is sent to the Imbalance Correction function, if not a FALSE condition is continuously sent.

In the Table 4, the inputs, outputs and parameters that need to be set within the Imbalance Observation function are presented:

Table 4. Inputs, outputs and parameters used for Imbalance Determination function of the Balance Restoration Control

Inputs	Outputs	Parameters
• $P_i^{TLsched}$ • P_i^{TLmeas} • f_{meas}	• PCE • Location • CCE	• $f_0 = 50Hz$ • $PCE^{Threshold}$ = (cell dependent)

2.6. Imbalance Correction

This function determines the reserve activation control signals based on the event location, Cell Control Error (CCE) and Power Control Error (PCE) value (depending on the type of resources) in order to correct the imbalance of the cell and the system frequency. The reserves list will determine the participation factor of each resource into the restoration process. The imbalance correction function developed integrates fast acting devices along with conventional generation for an improved effectiveness of fast acting devices (speed of response is not limited), it also allows for the activation of restoration reserves at the same time as containment reserves, improving the frequency response of the system.

For a faster but stable operation of the frequency restoration control, a parallel loop to conventional frequency restoration control (intended for conventional generation with limited ramp rates) with a faster PI control has been developed as shown in Fig.13. The combination of the fast and slow loop forms the Imbalance correction function. This, in contrast with the present Automatic Generation Control (AGC) control, allows for a stable and fast frequency restoration with an effective use of fast acting devices. Fast acting devices will only follow the reference from the fast PI once the frequency event has been located within the cell, this will allow for a localized response to local problems and at the same time avoids the impact that the miscalculation of the bias factor (typically defined based on experience) would cause during the restoration process.

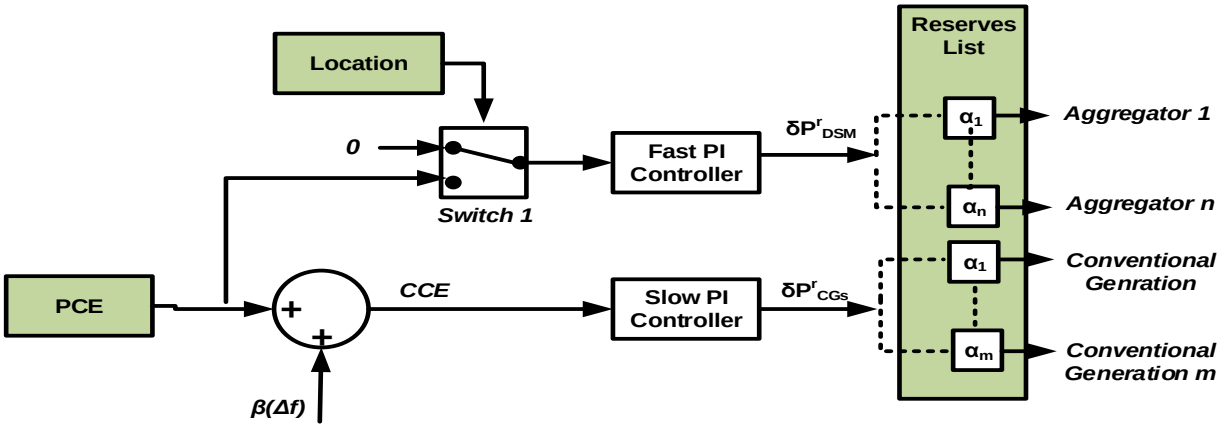

Figure 14. Imbalance Correction algorithm of the Balance Restoration Control

Table 5. Inputs, outputs and parameters used for Imbalance Correction function of Balance Restoration Control

Inputs	Outputs	Parameters	
• CCE • Location • Reserves final list	• Reserve activations, ΔP	• Fast PI: ○ K_{pf}, T_{if}	• Slow PI: • K_{ps}, T_{is}

2.7. Cell Set-point Adjusting

The functionality of the Cell Set-point Adjusting (CSA) is described below in a step-by-step algorithmic approach that for the two different variants, namely corrective and pre-emptive BSC.

A. Corrective version

1. It reads the vector of allowable tie-line deviations. This way it can calculate the limits of each tie-line so that the maximum allowable change can be estimated.
2. It remains standby until is triggered by a BRC output change. This means that the control function remains in a state in which it does not perform any action until it is triggered by an imbalance or by request by one of its neighbours.
3. It monitors the BRC output with a high sampling rate (1sec). The high sampling rate is necessary since the Rate-of-Change of BRC's output is used as a triggering signal. Unless the BRC output is monitored with a high sampling rate the derivative calculation may lead to incorrect results and early activation of BSC, before BRC has stabilized. In this case, it is possible to have adjustment at incorrect set-points that could lead to instability. Once an imbalance emerges, the BRC control function that corrects the imbalance should change its output. The output signal can be monitored by the CSA in order to estimate how much the activation of imbalance was and, thus, how much of imbalance power can be corrected by changing the set-points of the tie-lines. The ultimate goal of CSA is to detect imbalance above a specific threshold, hence, when BRC is higher than this threshold. This assumption is used in order to avoid continual modifications of the set-points of the tie-lines, which, eventually, may lead to BRC instability. Therefore, the BSC approach is used to modify set-points only in exceptional cases with rather large imbalances in order to partly free up the used BRC resources.
4. If the rate-of-change of the BRC output is less than a value (i.e. BRC has stabilised) it uses the final BRC value as an imbalance estimation. This quantity is used because it indicates that the BRC controller has stabilised its output and the balance has been restored. At this point, the CSA can identify how much BRC reserve power is being used to restore the cell balance. Evidently, this power is approximately equal to the imbalance. Therefore, the use of this information specifies how much the set-point can be modified in order to deactivate the used BRC reserves. This is the exact time when a good estimation of the imbalance can be made. The accuracy of this estimation depends on the accuracy of the BRC actions. Factors such as nonlinearities between the BRC signals and the actual power provided by the BRC reserves mean that the BRC output may not precisely correspond to the imbalance. However, this is not a crucial factor because the aim of BSC is only to optimise the use of BRC reserves. Therefore, some discrepancies would simply lead to a small deviation in the deactivation of the BRC reserves.
5. It compares the imbalance with all allowable tie-line deviations. This is due to the fact that the CSA controller has to determine which tie-lines can accept and how much of this adjustment. It is worth noting that the adjustment of the tie-lines should be done only if the imbalance from

step 4 is above a substantial limit in order to avoid continuous changes in the tie-line set-points even at the slightest imbalances.

6. If the imbalance is less than a safety margin (e.g. 20% under the maximum theoretical allowable deviation), it will issue to the corresponding neighbour the total imbalance as request for potential tie-line change. The reason for selecting a margin, as an example here at 80% of the maximum tie-line capacity is in order to ensure the tie-line will have some remaining capacity in case of a subsequent imbalance. Also, it should be pointed out here that the adjustment of the tie-lines set-points in this approach is valid no longer than one single timeframe, i.e. 15min. For the next time frame the whole procedure has to be repeated by considering the updated schedules of the tie-lines, which can have this adjustment incorporated.
7. For cells interconnected via one single tie-line if the imbalance is above the safety margin (80% or less of the allowable line capacity), the safety margin is selected as the requested adjustment value to the corresponding neighbour. For multiple tie-lines between two cells, the requested adjustment is proportionally distributed to the tie-lines based on their available capacity. In this case, this 80% limitation is again used to avoid overloading of the lines. This means that even if the imbalance is higher, the correction requested by the CSA should always be limited to the tie-line's margin.
8. After finishing steps 6 and 7 for all tie-lines it compiles an array of requested corrections and issues the relevant element of the array to the corresponding neighbour. This means that each neighbour should receive a different correction request.
9. If one neighbour responds with an acceptable value of correction, then a final reassessment of the BRC output is immediately done. In order for the neighbouring CSA to respond to the request, it must have undergone all steps from 1 to 4.
10. The current imbalance estimation based on the updated BRC output value is sent as final value of setpoint adjustment to the neighbour and to the function that observes imbalance. This means that the initial CSA which requested the adjustment should make a final check of the BRC output for potential changes and will send the final adjustment value if it is less than the response of the second controller.
11. If the function receives a request by another peer for changing the set-point of its tie-lines, it remains standby until an imbalance of the opposite sign takes place within it. This means that it will respond only if the actions of step 3 and 4 happen. Apparently, if the peer cell has already had an opposite sign imbalance it will respond immediately. In this case, the neighbouring cell would already be in the state of step 8.
12. If an imbalance happens, it performs steps 3-5.
13. It repeats step 6 but only issuing the corresponding value to the one that requested the adjustment. The value of adjustment should be selected as the minimum of the two imbalances.
14. Once it receives the final settled value from the neighbouring controller it repeats step 10 only for the function that observes imbalance.

The flowchart of Fig. 15 provides an overview of the execution of all above steps in all possible states of one cell.

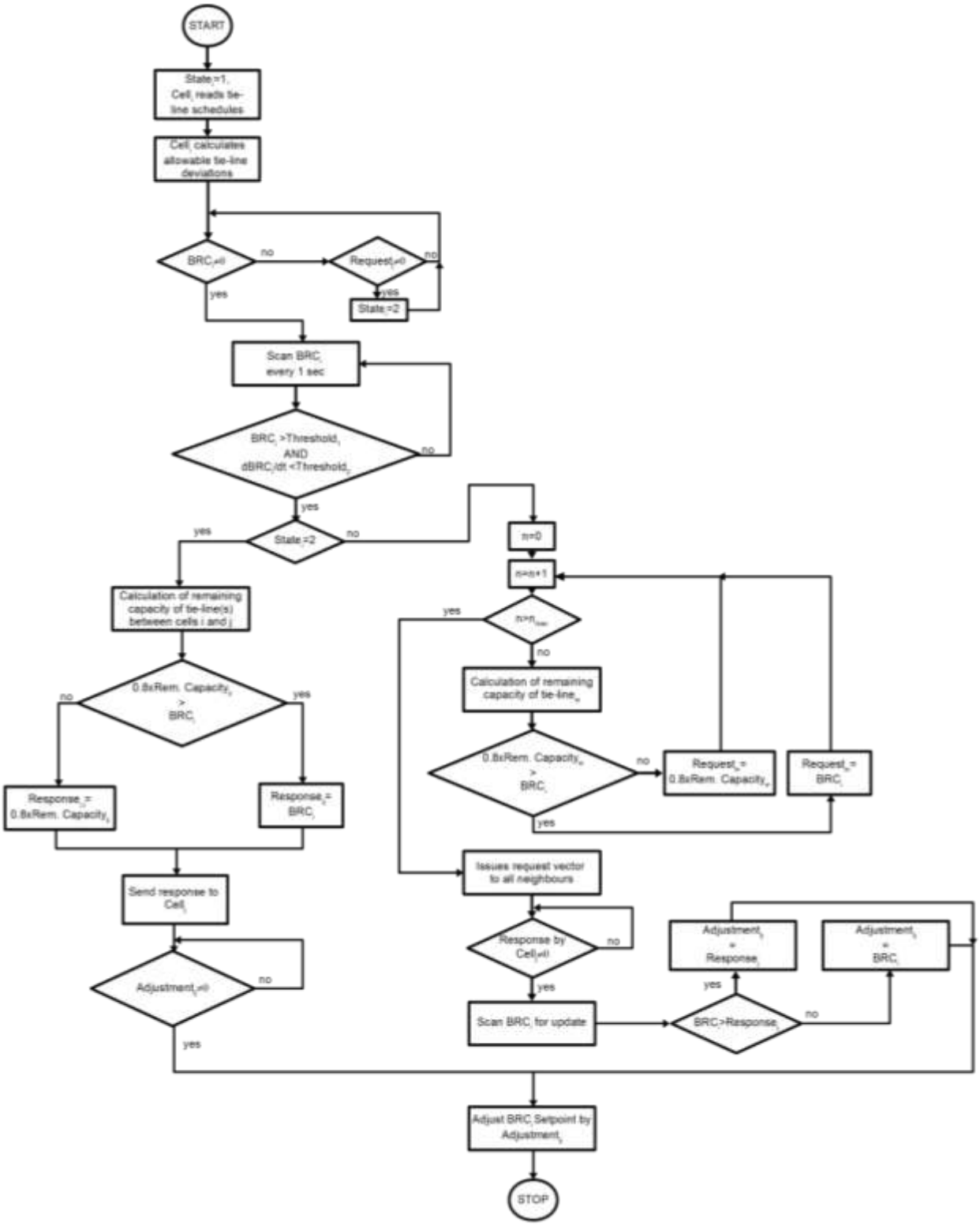

Figure 15. Flowchart of the corrective Cell Set-point Adjusting function operation

B. Pre-emptive version

This version presents a lot of similarities with the above one. Thus, the explanations of the corrective version are more or less the same. The major difference in this version is that it presumes a delayed activation of BRC. This means that BRC does not change anything before the

BSC actions attempt to modify the set-point of the tie-lines. In this case, it is not possible to use the output of the BRC controller in order to estimate the imbalance, but there has to be made use of signals from the frequency and tie-line measurements together with the Cell Power-Frequency Characteristic in order to calculate the imbalance based on the formula explained below:

1. It reads the vector of allowable tie-line deviations, similarly to step1 of the corrective version.
2. It reads the scheduled CPFC value. This can be used together with the frequency measurement in order to estimate which part of the imbalance is covered internally (by FCC resources within the cell).The second part of the imbalance is covered by the neighbouring cells via tie-lines power changes. Therefore, the controller can obtain an estimation of the imbalance by combining the two measurements as explained in step 6.
3. It remains standby until it is triggered by an imbalance which leads to tie-line/frequency changes.
4. It monitors the frequency and imbalance with a high sampling rate (1sec). This is done in order to estimate when the system has settled on a new stable state and after that to calculate the imbalance based on the frequency and tie-line power deviation.
5. If the rate-of-change of frequency (ROCOF) is less than a value (i.e. system has stabilised in a new frequency but not with the activation of BRC reserves yet), it uses the final delta_f and delta_Ptieline values for imbalance estimation. While the frequency indicates the amount of internal resources, the tie-line power deviation gives the amount of power interchanged in order to cover the imbalance.
6. It calculates (estimates) imbalance based on the formula Imbalance = $\Sigma\Delta P_{tie,i}$+CPFCΔf. After this calculation, all other steps are identical with the corrective version.
7. It compares the imbalance with all allowable tie-line deviations.
8. If the imbalance is less than a safety margin (e.g. 20% under the maximum theoretical allowable deviation), it will issue to the corresponding neighbour the total imbalance as request for potential tie-line change.
9. If the imbalance is above the safety margin, the safety margin is selected as request to the corresponding neighbour.
10. After doing steps 6 and 7 for all tie-lines it compiles an array of requested corrections and issues the relevant element of the array to the corresponding neighbour.
11. If one neighbour responds with the acceptable value of correction, then a final reassessment of the BRC output is immediately done.
12. The current BRC output is sent as final value of correction to the neighbour and to the function that observes imbalance.
13. If the function receives a request by another peer for imbalance correction it remains standby until an imbalance of the opposite sign takes place within it.
14. If an imbalance happens it performs steps 3-5.
15. It repeats step 6 but only issuing the corresponding value to the one that requested the correction. The value of correction should be selected as the minimum of the two imbalances.
16. Once it receives the final settled value from the neighbouring controller it repeats step 10 only for the function that observes imbalance.

2.8. Tie-line Limits Calculation

The specific function performs a simple calculation of the remaining available capacity of the tie-line to inform the Cell Set-point Adjuster functions of the capability of change in case of imbalance.

1. Receives the values of power schedules of the tie-lines corresponding to the beginning of the selected timeframe.
2. It retrieves the static information regarding the maximum power limits of the tie-lines.
3. It subtracts the scheduled powers from the maximum ones to calculate the difference (allowable power changes).
4. It issues the vector of allowed change to the Cell Set-point Adjuster together with the identity of each tie-line.

2.9. df/dt Droop Slope Determination

Note: this function is sometimes referred to as “Cell-level inertia dispatch function”.

This cell central function receives the inertia set-point from the synchronous area inertia controller. The inertia set-point should be respected for the next time window (assumed as the market time window). Based on different parameters, the cell-level inertia dispatch function determines the devices to participate in the inertia response control (IRPC) to respect the received set-point.

The inertia services could be delivered as synchronous inertia (via rotating machines) as well as synthetic inertia (e.g. via energy storages). It´s assumed that the synchronous inertia could be delivered only by means of synchronous generators or rotating condensers, which do not have as primary objective the provision of inertia services. In other words, their inertia value is considered once those are connected, regardless of the price.

The dispatch function receives the inertia set-point and check the inertia of the connected rotating machines. The residual inertia value is achieved by synthetic inertia devices, which are chosen in function of the price.

The function has two inputs. The first input is the cell inertia set-point and the second input is composed by a five column matrix, the lines correspond to the number of the devices which might participate in IRPC. The first column indicates the available/non available state of the device. The second indicates the inertia type (synchronous/synthetic). The third column indicates the inertia value of the device (in case of synthetic inertia, an equivalent inertia value should be provided). The fourth column indicates the service´s price, which is considered only in case of synthetic inertia. The last column is an index value used for the coding purpose.

The function has as output a vector which is communicated to the pool of devices able to participate in the IRPC. It´s a yes/no signal, it establishes the participation of the device or not in the IRPC for the next time window.

- **Input:**
  - The cell inertia set-point
  - Set of available devices with the following details
    - Available/non available status
    - Synchronous/synthetic inertia
    - The inertia value
    - The service’s price
    - Index value used for a coding purpose
- **Output:**
  - Device inertia set-point in the next time window (1 or 0 signal)

2.10. Post-primary Voltage Controlling function

The Post-primary Voltage Controlling function has two different tasks assigned:

1) Checks the current voltage values in the nodes to determine if they are within the regulatory safe band, and, if necessary, triggers the operation of the Post-primary Voltage Set-point Providing function.
2) Receives the calculated set point values by the Post-primary Voltage Set-Point providing function and sends it to the different devices.

The full procedure to perform the task 1) is represented graphically in Fig.16 and follows the sequence below:

1.1) The Post-primary Voltage Controlling function receives the magnitudes of the voltages in the nodes (input) continuously that are send by the measurement devices at a specific sampling ratio (e.g. 48 samples/cycle for PMUs).

1.2) It compares, for any node, the voltages measured with the stored values of maximum and minimum voltage levels allowable according to the regulation and standards in force.

1.3) Sends a binary signal (0/1) to the “Voltage_error” block for every comparison performed. If a node is out of the limits, it sends a FALSE signal (not in the safe band).

1.4) If the result of any comparison is FALSE, the function sends a trigger signal to the Post-primary set-point Providing Function (output).

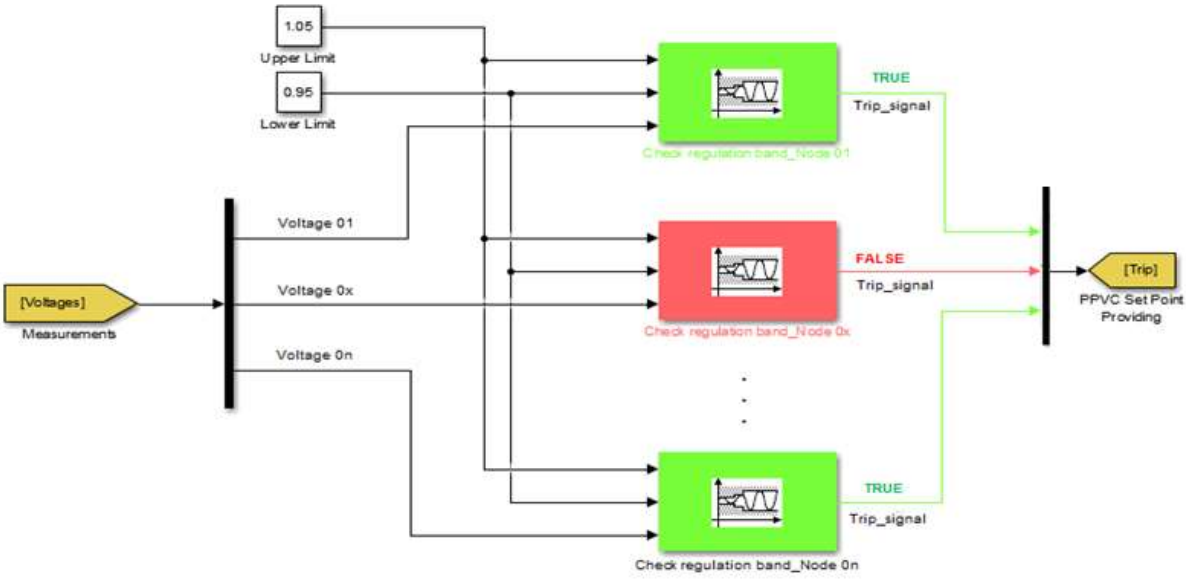

Figure 16. Post-primary Voltage Controlling Function. Task 1: Operation scheme

In the second task, the function does not execute any operation but acts only as an information hub:

2.1) It receives the set-point values calculated by the Post-primary Set-point Providing function.

2.2) It distributes the set-points to the different PPVC devices.

2.11. Post-primary Voltage Set-point Providing function

The objective of this function is the calculation of the optimal control variables in order to minimize the power losses in the grid. It is a function executing a classical optimal power flow (OPF) algorithm in the WoC context. The goal of the OPF is to get the optimal voltage set-points for the power system that satisfies some constraints and minimizes the objective function considered.

The general problem to be solved can be formulated as shown below. The mathematical reasoning presented here is based on the work in [2] and [3]:

- **Objective function**: minimization of the active power losses, shown in Eq. 22:

$$\min \sum_{i=1}^{N}\sum_{j=1}^{N} G_{ij}\left[\left(e_i - e_j\right)^2 + \left(f_i - f_j\right)^2\right] \quad (22)$$

Where the voltages in terminal nodes *i* and *j* are $\underline{V_i} = e_i + jf_i$ and $\underline{V_j} = e_j + jf_j$ and *Gij* is the conductance between nodes *i* and *j*.

The **variables** in an OPF algorithm can be classified into three main groups [ref]:

- *Control or decision variables*: all the variables that can be modified to fulfill the generation and load balance according to the problem restrictions. Some of these variables normally employed are: the P and the Q in the generators (or the P and the V in some cases), the tap position of the transformers and the capacitance/reactance of shunts or the phase shifter transformers angle.
- *State variables*: Those variables that represent a unique state of the system and describe the response of the system to changes in the control variables, e.g. the magnitudes of the voltages in the nodes without generators and the angles (except the angle of the slack bus)
- *Output variables*: Variables that are combined in non-linear expressions from the control and the state variables, such as the power flows in the lines.

There are also some other magnitudes that are constant. They are also known as demand variables. These are, for example, the active and reactive power of the loads that are known by the forecasts or other magnitudes that are variables that could also be controlled, but they are not due to several operational reasons, e.g., the active power P in a PV node that is not allowed to move.

The **restrictions** settling the boundaries for the solution are:

- Equality constraints: involve the power active and reactive balance equations, shown in Eq. (23) and Eq. (24).

$$P_{gi} - (1-\emptyset_i)P_{ci} - V_i^2\sum_{j\in N_i}\left(G_{sij} + G_{ij}\right) + \sum_{j\in N_i}\left[\left(e_i e_j + f_i f_j\right)G_{ij} + \left(f_i e_j + e_i f_j\right)B_{ij}\right] = 0 \quad (23)$$

$$Q_{gi} - (1-\emptyset_i)Q_{ci} + V_i^2\left[B_{si} + \sum_{j\in N_i}\left(B_{sij} + B_{ij}\right)\right] - \sum_{j\in N_i}\left[\left(e_i e_j + f_i f_j\right)B_{ij} + \left(e_i f_j + f_i e_j\right)G_{ij}\right] = 0 \quad (24)$$

Where P_{gi} and Q_{gi} are the active and reactive power of the generators, P_{ci} y Q_{ci} are the active and reactive power of the loads, B_{si} is the shunt susceptance at bus i, G_{sij} and B_{sij} are the conductance and the susceptance of the branches linking *i* and *j*, and $\emptyset_i$ represents the percentage of load that is available for load shedding.

- Inequality constraints: that can be both operational (to ensure a safe solution for the system) or physical limits of equipment, such as the active or reactive limits of the generators, maximum current that can circulate in the branches (I_{ij}^{max}), the limits in the

number of taps (r_i^{min} / r_i^{max}) or boundaries to the reactances of the shunts (x_i^{min} / x_i^{max}), (Eq. (25) to Eq. (31)):

$$\left(G_{ij}{}^2 + B_{ij}{}^2\right)\left[\left(e_i - e_j\right)^2 + \left(f_i - f_j\right)^2\right] \le \left(I_{ij}^{max}\right)^2, \ i,j = 1\ldots n \tag{25}$$

$$\left(V_i^{min}\right)^2 \le e_i{}^2 + f_i{}^2 \le (V_i^{max})^2 \tag{26}$$

$$P_{gi}^{min} \le P_{gi} \le P_{gi}^{max} \tag{27}$$

$$Q_{gi}^{min} \le Q_{gi} \le Q_{gi}^{max} \tag{28}$$

$$r_i^{min} \le r_i \le r_i^{max} \tag{29}$$

$$x_i^{min} \le x_i \le x_i^{max} \tag{30}$$

$$\emptyset_i^{min} \le \emptyset_i \le \emptyset_i^{max} \tag{31}$$

The resolution of the OPF problem is done by using the interior point methods (IPMs). The IPMs are widely used due to their speed of convergence and their robustness, so they do not need a very accurate initial point to reach the solution.

The OPF problem stated above can be written in a compact way as a general non-linear programming problem:

$$\min f(x) \tag{32}$$

Subject to

$$g(x) = 0 \tag{33}$$

$$h(x) \ge 0 \tag{34}$$

The **IPM algorithm** comprises four steps in order to get the optimal conditions:

1) Add slack variables (s_i) to the inequality constraints in order to convert them to equality and non-negative constraints.

2) The inequality constraints are then added to the original objective function, resulting in the optimization problem:

$$\min f(x) - \mu \sum_{i=1}^{q} \ln s_i \tag{35}$$

$$g(x) = 0 \tag{36}$$

$$h(x) - s = 0 \tag{37}$$

$$s \ge 0 \tag{38}$$

Where μ is a parameter that gradually decreases in the iteration process (barrier parameter).

3) Then, the equality constrained optimization problem is converted into a non-constrained one by defining the Lagrangian.

$$L_\mu(y) = f(x) - \mu \sum_{i=1}^{q} \ln s_i - \lambda^T g(x) - \pi^T [h(x) - s] \tag{39}$$

Where the vectors λ and π are the Lagrange multipliers.

4) Finally, the optimality conditions of the resulting problem are obtained by making zero the derivatives of the Lagrangian with regards to the all unknown values.

$$\begin{bmatrix} \nabla_s L_\mu(y) \\ \nabla_\pi L_\mu(y) \\ \nabla_\lambda L_\mu(y) \\ \nabla_x L_\mu(y) \end{bmatrix} = \begin{bmatrix} -\mu e + S\pi \\ -h(x) + s \\ -g(x) \\ \nabla f(x) - J_g(x)^T \lambda - J_h(x)^T \pi \end{bmatrix} = 0 \quad (40)$$

After the conditions have been adapted, it is necessary to define the search direction, the step size, the stop criteria and the updating process of the barrier parameter to apply a certain IPM algorithm.

Some of the most widely used IPMs are the Primal Barrier, the Primal-Dual and the Corrective-Predictive algorithms. Among all these algorithms, the Primal-Dual is the one used for the validation and implementation of the PPVC Use Case in a first approach and it is the one to be detailed in this document. However, multiple possibilities of IPMs (Primal Barrier, Predictor-Corrector, etc.) could be considered as well as other type of algorithms, such as genetic or evolutionary algorithms.

The full sequence to apply the Primal-Dual algorithm can be summarized in some steps as follows [3], [3]:

1) Set iteration k = 0 and $\mu^0 > 0$. Initialize y^0 considering that (s^0 and π^0) > 0.
2) Solve the conditions for the Newton direction Δy^k

$$H(y^k) \begin{bmatrix} \Delta s^k \\ \Delta \pi^k \\ \Delta \lambda^k \\ \Delta x^k \end{bmatrix} = \begin{bmatrix} \mu^k e - S^k \pi^k \\ h(x^k) - s^k \\ g(x^k) \\ -\nabla f(x^k) - J_g(x)^T \lambda^k - J_h(x^k)^T \pi^k \end{bmatrix} \quad (41)$$

3) Determine the maximum step length $\alpha^k \in (0,1)$ in the Newton direction Δy^k such as (s^{k+1} and π^{k+1}) > 0.

$$\alpha^k = min\left\{1, \gamma \min_{\Delta s_i^k < 0} \frac{-s_i^k}{\Delta s_i^k}, \gamma \min_{\Delta \pi_i^k < 0} \frac{-\pi_i^k}{\Delta \pi_i^k}, \right\} \quad (42)$$

4) Check convergence: if objective function between two consecutive steps below the established tolerances, the calculation process stops.
5) If convergence not achieved, update the barrier parameter $\mu^{k+1} = \sigma \rho^k / q$, where σ is usually set to 0.2 (in any case between 0 and 1). *k=k+1* and repeat from step 2.

3 White box descriptions of essential auxiliary functions

Some functions that are strictly spoken not in scope of IRP ELECTRA, but are still very important for the experimental testing of use-cases are included in this document. They are important for the related simulations and in particular the lab-scale experiments within ELECTRA. Those functions which belongs to the higher Control topology levels (CTL2 or CTL3), are in focus in the simulations and in the validations, but CTL0 functions cannot be fully neglected in simulations or in lab experiments, because those functions must be implemented and those are the ones delivering the service. The motivation for this is given in italics at the beginning of each paragraph.

3.1 Cell Inertia Setpoint Provider

Reason for presence in this document: This function was originally considered as out of ELECTRA scope function, but Electra focuses on functions in CTL2 and CTL3 and to create a complete model and the relations/connections among the functions in the (IRPC) Inertial Response Power Controller Uce Case, the cell inertia set-point provider is implemented.

This central function determines the inertia set-point (Js) to be respected on the synchronous area level and communicates to each cell their relative requested inertia set-point.

The function has three inputs, the maximum power mismatch (delta P %) for which the grid should be able to operate in secure state, the ROCOF limit to be respected and a vector with the installed power of the different cells.

Based on the swing equation, the J_{tot} gets calculated as following:

$$J_{tot} = \frac{\Delta P}{(2*\pi)^2 * 2f * \frac{\Delta f}{\Delta t}} \tag{43}$$

Afterwards the function dispatches the J_s over the cells communicating to each cell the requested inertia value. The inertia set-point is calculated in function of the installed power of each cell as a weighted average

$$J_{cell-i} = \frac{J_{tot} * P_{cell-i}}{P_{tot}} \tag{44}$$

Input:

- The maximum power mismatch (ΔP%)
- RoCoF limit
- Installed power from the different cells (P_{cell-i})

Output:

- A vector with the inertia set-point requested from each cell J_{cell-i}

3.2 Rate of Change of Frequency Observer

Reason for presence in this document: This function was originally considered as out of ELECTRA scope function, since it is on CTL0. To highlight the effects and characteristic of Rate of Change of Frequency Observer, the function is implemented. It is important in simulations and on which WP7 experiments are based. We cannot neglect completely CTL0 in simulations or in lab experiments because those functions must be implemented and those are the ones delivering the service.

Rate of change of frequency observer is function continuously sampling voltage waveforms to calculate the local frequency and the rate of change of the frequency (ROCOF). This can be at either the connection point of a single device or a Point of Common Coupling of the aggregated resource.

It has as input the voltage waveforms and calculates the frequency. It has been used a Phase Lock Loop (PLL), which track the frequency and phase of a three-phase signal by using an internal frequency oscillator.

The ROCOF is calculated over 200 ms based on 100-ms moving window.

The measuring window is defined as the number of power frequency measuring periods over which the rate of change of frequency is calculated:

$$\frac{\Delta f}{\Delta t} = \frac{1}{5}\sum_{i=1}^{5}\frac{\Delta f_i}{\Delta t_i} \quad (45)$$

Δf_i the frequency variation within one cycle
Δt_i the cycle's duration

Input

Voltage waveforms

Output

Frequency
Delta f/delta t.

3.3 Inertia Response Power Controller

Reason for presence in this document: This function was originally considered as out of ELECTRA scope function, because it is on CTL0 but to create a more complete image of all the use case (IRPC), the Inertial Response Power Controller function is implemented, otherwise we are unable to provide this service and implement it in simulation and in the lab.

This function increases or decreases active power generation or consumption in a manner proportional to the locally observed ROCOF. It has as input the ROCOF ($\Delta f_{loc}/\Delta t$) and the activation signal and as output the increased/decreased active power generation/consumption (continuously). The function is based on a proportional controller.

For simplification, as first assumption the device inertia set-point is considered as yes/no signal, which indicates if the device will participate in the inertia control or not for the next time window (e.g. next 15 min). Therefore, it is assumed that the equivalent inertia of the device is known a priori.

To include the device dynamics (e.g. the battery) a rate limiter and time delay blocks are considered.

Input:

- $\frac{\Delta \mathbf{f}}{\Delta \mathbf{t}}$
- Device participation or not in the next time window (1/0 signal)

Output:

- Active power consumption or generation

3.4 Policy Calculation

Reason for presence in this document: This white-box function will be used to support the 'balance merit order decision function'. The simulations performed here will ensure a successful implementation of 'balance merit order decision function'.

This function works in the reserve scheduling phase and the function will be used by cell operator to make the reserve available. Inspired by the PJM Reg A and Reg D market setup, two types of BRC regulation signals are considered here, namely slow regulation signal and fast regulation signal. Two types of resource providers are assumed to be available in this cell, the slow generation units that mainly follows the slow regulation signal and the batteries that mainly follow the fast regulation signal. To allocate the basic schedule and reserves, a cost function for the slow generation unit and battery is defined as follows:

The cost function of slow generation (GS) unit:

$$f_1\left(P^{GS}(\delta_1)\right) = \alpha^{GS}\left(P_{Sch}^{GS} + R^{GS}\delta_1\right)^2 + \beta^{GS}\left(P_{Sch}^{GS} + R^{GS}\delta_1\right) + C_{GS} \quad (46)$$

s.t. power constraint, ramping constraint.

Where P_{Sch}^{GS} is the day ahead schedule of the slow generation unit, R^{GS} is the BRC reserve, δ_1 is the energy content of the slow regulation signal, $\alpha^{GS}, \beta^{GS}, C_{GS}$ are coefficients of the cost function.

The cost function of battery unit:

$$f_2\left(P^{BAT}(\delta_2)\right) = \beta^{BAT}(P_{Sch}^{BAT} + R^{BAT}\delta_2) \quad (47)$$

S.t. power constraint, energy constraint.

Where Where P_{Sch}^{BAT} is the day ahead schedule of the battery unit, R^{BAT} is the BRC reserve, δ_2 is the energy content of the fast regulation signal, β^{BAT} is the coefficient of the cost function.

These cost functions will be made available to cell operators who will then make a centralized dispatch with the objective of minimizing the operational cost as well as respecting the constraints. The overall optimization is formulated as follows:

$$E_{\delta_1,\delta_2}\{f_1 + f_2\} \quad (48)$$

S.t. to local constraints of each units, global constraints such as cell power balance, cell network security constraint etc.

By solving this robust optimization, the cell operator defines the reserves (R^{GS}, R^{BAT}) for each unit. Note here, for each type of unit, we assume that many resources are available. Here, the reserves are also called policies which will be used in the real-time operation phase.

3.5 PVC Controller

Reason for presence in this document: This function was considered as out of ELECTRA scope function, This function is responsible for fast voltage control and also acts as an actuator for PPVC, therefore it is necessary to implement it so that simulations (of other use-cases) can be performed.

PVC Controller is the main function of Primary Voltage Control. Since a high number of different solutions for voltage controllers exist already, and the controller configuration and its parameters are highly dependent on the type of device that the controller operates on, the purpose of this controller design is to be as generic and flexible as possible. Specific alterations can be made if needed by application. This is a generic function in order to allow for running tests of the remaining control schemes as well as testing the other function of the PVC, which is the grid impedance

estimator.

The structure of the controller is depicted in figure 17. A basic feedback loop is represented. The main part is embedded in *Regulator* block which can include any kind of a transfer function shaping the dynamic response of the control loop.

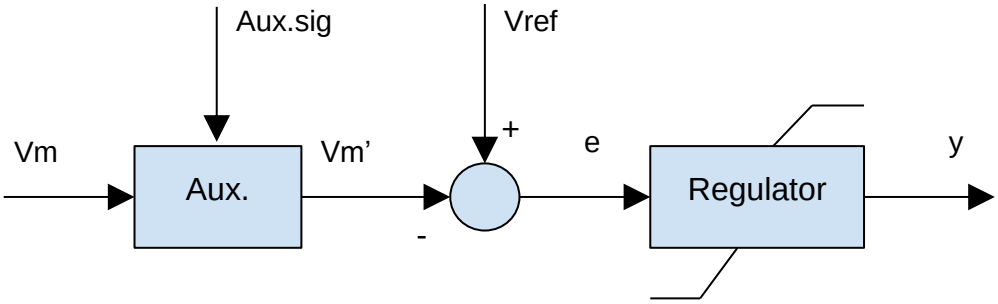

Figure 17. Structure of PVC Controller

In this use case a PI regulator is implemented. Its operation is defined by the following equation,

$$y = k_p \cdot e + k_i \cdot x_{PI} \tag{49}$$

where x_{PI} is the state variable of the integrator and e is the control error. The control error is a difference between the reference voltage V_{ref} (e.g. 1 pu) and measured voltage V_m converted by the function *Aux.* to signal V_m'. Output signal y from the regulator is constrained to lower and upper bounds. K_p and k_i are the gains of the controller.

Function *Aux*. allows for three basic modes of operation:

1. Direct feedthrough of signal V_m to signal V_m', so that $V_m' = V_m$,
2. Line drop compensation
3. Droop control

Ad.2. Line drop compensation

This mode allows for controlling voltage in a different point than the measurement point, for example it can be a virtual point inside the step-up transformer or some point in the middle of a long radial line.

Line drop compensation works according to the following equation,

$$V_m' = V_m - \kappa \cdot X_T \cdot I_Q \tag{50}$$

Where X_T is the reactance between the source and the power system, I_Q is the reactive current of the source (auxiliary signal) and κ is the coefficient that allows to choose the exact location of the voltage control point. The principle of line drop compensation is depicted in Figure 18.

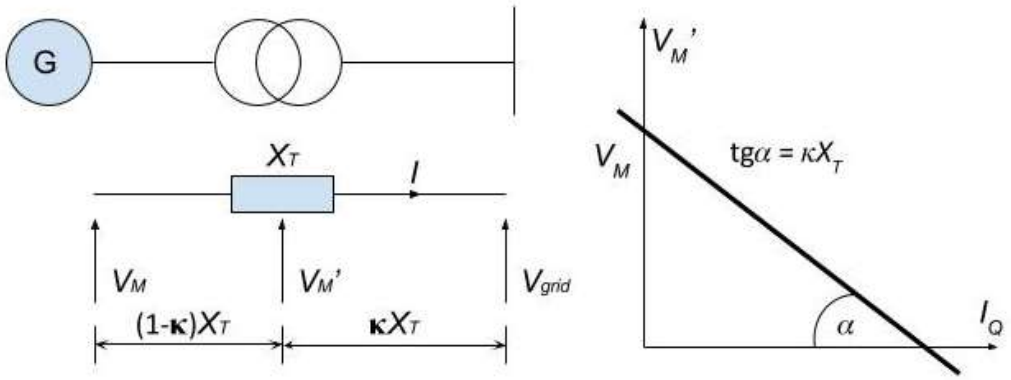

Figure 18. Principle of line drop compensation

Ad.3. Droop control

This mode allows for droop operation, which is useful when several units control voltage at the same location or when a tradeoff between the steady-state accuracy and reactive power reserves is needed.

The droop is implemented via the following formula,

$$V_m' = V_m - k_Q \cdot Q \tag{51}$$

Where Q is the reactive power and k_q is the droop coefficient. In some applications current instead of reactive power can be used as a feedback signal in the droop control.

Equations (50) and (51) indicate a similarity between the two available methods. The main difference between them consists in the fact that in the line drop compensation method a regulation point can be selected. In the droop control the focus is on relaxing the accuracy of the controller thus freeing reactive power reserves.

3.6 Grid Impedance Estimator

Reason for presence in this document: This function was considered as out of ELECTRA scope function and it is not mentioned in the Electra deliverable D4.2. PVC is designed in a way that it is universal for all voltage levels (i.e. grid types). But especially on the low voltage level active power is also used for voltage control and therefore it is necessary to know what is the characteristics (X/R ratio) of the grid at the point of common coupling. Grid Impedance Estimator performs this task as a supplementary function of the PVC Controller otherwise we are unable to provide this service and implement it in simulation and in the lab.

Introduction

Grid Impedance Estimator (GIE) is a function of the PVC responsible for the current estimate of a value of the grid substitute impedance. The structure of a grid reduced to a basic two-bus network is depicted in figure 19. Z_L is the impedance of the grid seen from the generating bus.

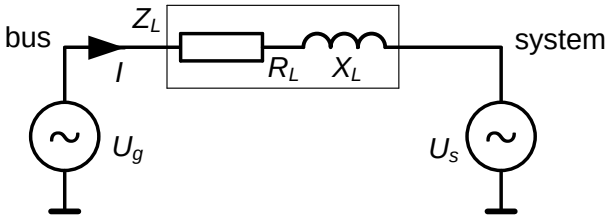

Figure 19. The structure of a grid reduced to a basic two-bus network

The structure from the Fig 19 can be described by the following equation,

$$Ug = Us + I\cdot(R_L + iX_L), \quad (52)$$

where phasors of voltage and current: $\underline{U_g}, \underline{U_s}, \underline{I} \cdot \in C$,

$$RL = \Re(ZL), \quad XL = \Im(ZL).$$

The equation (52) can be transformed to:

$$\Re Ug = \Re Ug + \Re I\cdot RL + \Im I\cdot XL, \quad (53a)$$

$$\Im Ug = \Im Ug + \Im I\cdot RL + \Re I\cdot XL. \quad (53b)$$

Let:

$\underline{U_g}[n]$ - will be the last measured phasor of voltage at the bus,
$U_g[n-k]$ - the k-previous value, for the time $t\text{-}k\cdot T_p$,

where: t – current time, T_p – sampling time, $k \in \{1,2, \ldots k_{max}\}$, and:

$U_{gkr} = \Re\underline{U_g}[n-k]$ - real part of the k-previous value of $\underline{U_g}$,
$U_{gki} = \Im\underline{U_g}[n-k]$ - imaginary part of the k-previous value of $\underline{U_g}$,
$U_{skr} = \Re\underline{U_s}[n-k]$ - real part of the k-previous value of $\underline{U_s}$,
$U_{ski} = \Im\underline{U_s}[n-k]$ - imaginary part of the k-previous value of $\underline{U_s}$,
$I_{kr} = \Re\underline{I}\,[n-k]$ - real part of the k-previous value of $\underline{I}$,
$I_{ki} = \Im\underline{I}\,[n-k]$ - imaginary part of the of $\underline{I}$.

then for the k-previous measured values the equation (53) takes the form:

$$Ugkr = Uskr + Ikr\cdot RL + Iki\cdot XL, \quad (54a)$$

$$Ugki = Uski + Iki\cdot RL + Ikr\cdot XL. \quad (54b)$$

The R_L and X_L for the k-previous measured values can be calculated as follows:

$$R_L = \frac{A_k}{C_k}, \quad (55a)$$

$$X_L = \frac{B_k}{C_k}, \quad (55b)$$

where

$$Ak = (Ugkr - Uskr)\cdot Ikr\cdot + (Ugki - Uski)\cdot Iki, \quad (56a)$$

$$Bk = (Ugki - Uski)\cdot Ikr\cdot - (Ugkr - Uskr)\cdot Iki, \quad (56b)$$

$$Ck = Ikr2\cdot + Iki2. \quad (56c)$$

It can be expected that measured values of voltage and current will be disturbed. Assuming that grid impedance is rather stable value that changes along with grid configuration changes, the grid impedance can be estimate with the use of several last measurements using least-squares method. The R_L and X_L with use of the k measurements can be calculated as follows:

$$R_L = \frac{\sum_{k=0}^{kmax} A_k}{\sum_{k=0}^{kmax} C_k}, \quad (57a)$$

$$X_L = \frac{\sum_{k=0}^{kmax} B_k}{\sum_{k=0}^{kmax} C_k}. \quad (57b)$$

While that grid impedance can change along with grid configuration changes, ability of following the current grid impedance value of the estimator formulas (57a, 57b) can be improved by introducing a forgetting factor λ. The formulas takes the form:

$$\mathrm{R_L} = \frac{\sum_{k=0}^{kmax} \lambda^k \cdot \mathrm{A_k}}{\sum_{k=0}^{kmax} \lambda^k \cdot \mathrm{C_k}}, \tag{58a}$$

$$\mathrm{X_L} = \frac{\sum_{k=1}^{kmax} \lambda^k \cdot \mathrm{B_k}}{\sum_{k=1}^{kmax} \lambda^k \cdot \mathrm{C_k}}, \tag{58b}$$

where: $\lambda \in (0, 1\rangle$**.**

Grid substitute impedance estimation seen from a generating bus

An assumption has been made, that measurements at the generating bus are available, both at the generator as well at the grid side transformer. It makes the described method independent of measurements at any other buses in grid and of difficulties arising from data transmission from distant buses.

The second assumption, a common one in this issue, is that values of substitute impedance of grid and substitute voltage of grid is stable in time of estimation.

$$\mathrm{Uskr} \approx \mathrm{const}, \quad \mathrm{Uski} \approx \mathrm{const} \tag{59a}$$

$$\mathrm{RL} \approx \mathrm{const}, \quad \mathrm{XL} \approx \mathrm{const}, \tag{59b}$$

Then for sufficient numbers of varying values of voltage and current at the bus a value of R_L and X_L can be estimated. For series of k=0..k_{max} measured values of U_{gkr}, I_{kr} the below relationships can be formulated.

$$\sum_{k=1}^{kmax} \left(\mathrm{U_{gkr}} - \mathrm{U_{skr}} - \mathrm{I_{kr}} \cdot \mathrm{R_L} + \mathrm{I_{ki}} \cdot \mathrm{X_L}\right) \cdot \lambda^k = 0, \tag{60a}$$

$$\sum_{k=1}^{kmax} \left(\mathrm{U_{gki}} - \mathrm{U_{ski}} - \mathrm{I_{ki}} \cdot \mathrm{R_L} - \mathrm{I_{kr}} \cdot \mathrm{X_L}\right) \cdot \lambda^k = 0, \tag{60b}$$

Bearing in mind (59ab), the relationships (60ab) can be formulated:

$$\sum_{k=1}^{kmax} \mathrm{U_{gkr}} \cdot \lambda^k - \mathrm{K_\lambda}^{-1} \cdot \hat{\mathrm{U}}_{\mathrm{sr}} - \hat{\mathrm{R}}_{\mathrm{L}} \cdot \sum_{k=1}^{kmax} \mathrm{I_{kr}} \cdot \lambda^k + \hat{\mathrm{X}}_{\mathrm{L}} \cdot \sum_{k=1}^{kmax} \mathrm{I_{ki}} \cdot \lambda^k = 0, \tag{61a}$$

$$\sum_{k=1}^{kmax} U_{gki} \cdot \lambda^k - K_\lambda^{-1} \cdot \hat{U}_{si} - \hat{R}_L \cdot \sum_{k=1}^{kmax} I_{ki} \cdot \lambda^k + \hat{X}_L \cdot \sum_{k=1}^{kmax} I_{kr} \cdot \lambda^k = 0, \tag{61b}$$

where: $K_\lambda^{-1} = \sum_{k=1}^{kmax} \lambda^k$,

and
- $\hat{U}_{sr}$ - U_{sr} estimate,
- $\hat{U}_{si}$ - U_{si} estimate,
- $\hat{R}_L$ - R_L estimate,
- $\hat{X}_L$ - X_L estimate.

With the use of least-square criterion estimation error can be minimized, then $\hat{R}_L$, $\hat{X}_L$ can be calculated according the formulas:

$$\hat{\mathrm{R}}_{\mathrm{L}} = \frac{\mathrm{A}}{\mathrm{C}}, \tag{62a}$$

$$\hat{\mathrm{X}}_{\mathrm{L}} = \frac{\mathrm{B}}{\mathrm{C}}, \tag{62b}$$

where:

$$A = K_\lambda \cdot \left(\sum_{k=1}^{kmax} U_{gkr} \cdot \lambda^k\right) \cdot \left(\sum_{k=1}^{kmax} I_{kr} \cdot \lambda^k\right) + K_\lambda \cdot \left(\sum_{k=1}^{kmax} U_{gki} \cdot \lambda^k\right) \cdot \left(\sum_{k=1}^{kmax} I_{ki} \cdot \lambda^k\right) - \sum_{k=1}^{kmax} U_{gkr} \cdot I_{kr} \cdot \lambda^k - \sum_{k=1}^{kmax} U_{gki} \cdot I_{ki} \cdot \lambda^k$$

$$\mathrm{B} = -\mathrm{K}_\lambda \cdot \left(\sum_{\mathrm{k=1}}^{\mathrm{kmax}} \mathrm{U_{gkr}} \cdot \lambda^{\mathrm{k}}\right) \cdot \left(\sum_{\mathrm{k=1}}^{\mathrm{kmax}} \mathrm{I_{ki}} \cdot \lambda^{\mathrm{k}}\right) + \mathrm{K}_\lambda \cdot \left(\sum_{\mathrm{k=1}}^{\mathrm{kmax}} \mathrm{U_{gki}} \cdot \lambda^{\mathrm{k}}\right) \cdot \left(\sum_{\mathrm{k=1}}^{\mathrm{kmax}} \mathrm{I_{kr}} \cdot \lambda^{\mathrm{k}}\right) - \sum_{\mathrm{k=1}}^{\mathrm{kmax}} \mathrm{U_{gkr}} \cdot \mathrm{I_{ki}} \cdot \lambda^{\mathrm{k}} - \sum_{\mathrm{k=1}}^{\mathrm{kmax}} \mathrm{U_{gki}} \cdot \mathrm{I_{kr}} \cdot \lambda^{\mathrm{k}}$$

$$C = K_\lambda \cdot \left(\sum_{k=1}^{kmax} I_{kr} \cdot \lambda^k\right)^2 + K_\lambda \cdot \left(\sum_{k=1}^{kmax} I_{ki} \cdot \lambda^k\right)^2 + \sum_{k=1}^{kmax} \left({I_{kr}}^2 + {I_{ki}}^2\right) \cdot \lambda^k$$

$$D = K_\lambda \cdot \left(\sum_{k=1}^{kmax} I_{kr} \cdot \lambda^k\right)^2 + K_\lambda \cdot \left(\sum_{k=1}^{kmax} I_{ki} \cdot \lambda^k\right)^2 - \sum_{k=1}^{kmax} \left({I_{kr}}^2 + {I_{ki}}^2\right) \cdot \lambda^k$$

Use of Grid Impedance Estimator

A necessary condition of proper determination of the substitute grid impedance, strictly – resistance and reactance, by the GIE algorithms is stable values of substitute impedance and substitute voltage of grid in time of estimation. In order to estimate grid impedance with satisfactory accuracy, sufficient numbers of varying values of voltage and current at the bus should be available. Usually minimal time of measurement do not exceed 1 sec. There are two circumstances in which the GIE algorithms can operate efficiently:

1. A change of current flowed from/to bus, usually with accompanying change of bus voltage took place, and it is known that it was not caused by a change of substitute grid impedance or voltage. For instance, transformer tap change occurred.
2. A change of bus current and voltage was caused for that purpose intentionally. It can be caused by a tap change of a transformer or a change of operation point of generator or load.

After proper estimation of grid impedance, the GIE algorithms are able to follow its changes.

A change of substitute voltage of grid, which can be caused i.e. by short-circuit, an outage of a generator or a load, disturbs online estimation of grid impedance. The GIE algorithm brings value of grid impedance up to date in a way described above.

Described features of the GIE algorithm enables using it at any bus which deals with at least one of the two situations described above.

4 Conclusions and next steps

This deliverable contains the detailed descriptions of the complete set of functions that are the building blocks for all the algorithms allowing for a consistent control of each cell within the Web-of-Cells. In addition to the core functions of use cases, the deliverable contains also the descriptions of some auxiliary functions. The last mentioned functions are important for related simulations and lab-scale validation of the control functions. Those functions belonging to the higher Control topology levels (CTL2 or CTL3), are in focus in the simulations and in the validations without

neglecting completely CTL0 functions in simulations or in lab experiments, because those functions must be implemented and those are the ones delivering the service.

The main outcome of the work reported in this document are the descriptions of the single core functions and of some auxiliary functions. The work reported in this deliverable included also the preparation of the software codes mainly Matlab scripts, but the codes are not presented in this deliverable. The simulations showed the proper functioning of the algorithms and codes. Moreover the document is evidence that the putting into simulations code of the functions was successful.

This document provides therefore a firm basis for the proof of the Web-of-Cells in the succeeding activities that target at simulation of the full Use-Cases in stand-alone mode and in combined mode as well as for the ultimate experimental validation. In the next stage, the single functions of each Use Case will be integrated into test network and the functionality in the stand-alone operation of the whole use-case will be proven in a representative test grid by simulations. Simulation of different scenarios and results will be compared against ENTSO-E Reference case. In the final stage, the testing and validation of combinations of Use Cases will be carried out. Multiple Use Cases will be integrated into test network and the functionality in combined operation of use-cases will be proven in representative test grids by simulations. The results of simulations will be compared against ENTSO-E Reference case to certain extent. Based on the results, selected functionalities and test scenarios will be transferred for validation by laboratory tests to partner laboratories.

5 References

[1] http://www.electrairp.eu (ELECTRA IRP web site)

[2] Capitanescu,F; Glavic,M.; Ernst,D.; Wehenkel,L. "*Interior-point based algorithms for the solution of optimal power flow problems"*, Electric Power Systems Research, Volume 77, Issues 5–6, April 2007, Pages 508-517, ISSN 0378-7796, http://dx.doi.org/10.1016/j.epsr.2006.05.003.

[3] Potra, F.A.; Wright, S.J.. "*Interior-point methods*". Journal of Computational and Applied Mathematics, Volume 124, Issues 1–2, 1 December 2000, Pages 281-302, ISSN 0377-0427, http://dx.doi.org/10.1016/S0377-0427(00)00433-7.

[4] Caerts, C., Rikos, E., Syed, M.,Guillo Sansano, E., Merino Fernandez, J., Rodriguez Seco, E., Evenblij, B., Rezkalla, M., Kosmecki, M., Temiz, A., Cabiati, M., Tornelli, C., Uslar, M., Heussen, K., Marinelli, M. 2017. *Description of the detailed Functional Architecture of the Frequency and Voltage control solution(functional and information layer).* Deliverable D4.2: Electra Project No. 609687, FP7-Energy-2013-IPR. European Commission. 115 p. http://www.electrairp.eu (ELECTRA IRP web site)

[5] Fisscher, K., Heussen, K., Hu, J., Hänninen, S., Rezkalla, M., D'hulst, R., Merino, J., Rodríguez, E., Rikos, E., Kosmecki, M. 2015. *Functional specification of the control functions for the control of flexibility across the different control boundaries*. Deliverable D6.1: Electra Project No. 609687, FP7-Energy-2013-IPR. European Commission. 85 p + Appendix 1, 46 p. and Appendix 2, 42 p. http://www.electrairp.eu (ELECTRA IRP web site)

[6] Caerts, C., D'hulst, R., De Breucker, S., Rikos, E., Kolodziej, D., Merino, J., Rodríguez, E., Heussen, K., Kok, K., Geibel, D., Tornelli, C.,Temiz, A. 2015. *Specification of Smart Grids high level functional architecture for frequency and voltage control. Deliverable* D3.1: Electra Project No. 609687, FP7-Energy-2013-IPR. European Commission. 112 p. http://www.electrairp.eu (ELECTRA IRP web site)

6 Disclaimer

The ELECTRA project is co-funded by the European Commission under the 7th Framework Programme 2013.

The sole responsibility for the content of this publication lies with the authors. It does not necessarily reflect the opinion of the European Commission.

The European Commission is not responsible for any use that may be made of the information contained therein.